GEOPHYSICAL RESISTIVITY INVESTIGATION OF WEATHERED BASEMENT OF ZAINAWA VILLAGE, KANO STATE, NIGERIA

BY

ALIYU NAFIU SADIQ

M.Sc./SCIEN/02829/08-09

A THESIS SUBMITTED TO THE POSTGRADUATE SCHOOL,

AHMADU BELLO UNIVERSITY, ZARIA

IN PARTIAL FULFILLMENT FOR THE AWARD OF THE DEGREE OF MASTERS OF SCIENCE IN APPLIED GEOPHYSICS.

DEPARTMENT OF PHYSICS

FACULTY OF SCIENCE, AHMADU BELLO UNIVERSITY, ZARIA

MARCH 2014

DECLARATION

I hereby declare that, this thesis is an original work carried out by me under the supervision of **Dr. A. L Aminu and Dr. Chiemeke Collins.**

To the best of my knowledge, no part thereof has been submitted elsewhere for the award of degree.

The works of others are duly acknowledged and referenced.

---------- ---------- ----------

Name of student Signature Date.

Author

DEDICATION

I dedicate this thesis to the Almighty ALLAH to whom my body and soul belong and also thank him for his immeasurable mercy showered on me.

CERTIFICATION

This thesis titled **"GEOPHYSICAL RESISTIVITY INVESTIGATION OF WEATHERED BASEMENT OF ZAINAWA VILLAGE, KANO STATE, NIGERIA "** by Aliyu Nafiu Sadiq, meets the regulations governing the award of the degree of Masters of Science(Applied Geophysics) of Ahmadu Bello University, Zaria and is approved for its contribution to knowledge and literary presentation.

_____ Date _____

Dr. Aminu A.L

Chairman, Supervisory committee

_____ Date_____

Dr. Chiemeke Collins

Member, Supervisory Committee

_____ Date_____

Dr. Sadiq U.

Head of Department of Physics

_____ Date_____

Prof. A.A Joshua

Dean, Postgraduate School

ACKNOWLEDGEMENT

My profound gratitude goes to Almighty ALLAH, the most beneficent, the most merciful, the first and the last, the sustainer, the retainer, the best planner, the best judge. May he grant paradise to those of us who believe in him till the last hour.

Its my pleasure to acknowledge the assistance of the following people who have contributed positively in one way or the other to the success of this study

My special gratitude goes to my supervisor Dr. Aminu A.L; who took me as his brother as well as his student and thoroughly supervised this work, always had time for me to give me some correction and words of encouragement during my studies and when I lost my mother.

I am highly indebted to Dr. C. Collins who is also my second supervisor. He supervised the field work and gave me all the necessary assistance both technical and material needed in the field work and the processing of the data. Sir, Thank you very much and may Almighty ALLAH reward you wherever you are.

I owe my unreserved gratitude to Dr. Sule P. who took his time and pain to explain in detail what resistivity is all about. Sir, I am very grateful for your intellectual guidance.

My gratitude also goes to my only course mate Mallam Abubakar Ibrahim who made available his car and accommodation during the field work.

I would like to acknowledge my late parents who laid down my educational foundation with their hard labour and unfortunately they could not reap from their hard labour. May Almighty ALLAH grant them paradise and reward them for their hard labour.

I appreciate the contribution made by my wife, my children (Abdulbaseet, Abdulmuqeet, Ize and Oyiza) for their patience and understanding during the period of my course.

I would not forget the sacrifice made by my sisters and my brothers to see that my second degree

became reality, especially when my beloved mother passed away.

ABSTRACT

The type of method adopted for this research was the 1D electrical resistivity, using the GEOPULSE SAS 300. A Schlumberger configuration was carried out to map the Geological feature of the earth subsurface. Five profiles were carried out in the study area. The layout geometry for the electrical resistivity was symmetrical Schlumberger arrays. The maximum current electrode separation (AB) was 140m, that is, AB/2=70m. The data obtained using Geopulse resistivity Meter SAS 300 were processed using computer software (IPI2Win). 30 vertical electrical soundings have been carried out that is each profile consists of six(6) vertical electrical soundings.

Based on the electrical resistivity value obtained in the study area, the following deductions were made.

The average depth to the fresh basement is about 29.8m. The study area has revealed the presence of two distinct layers, the top soil and weathered basement; the top soil is composed of laterite and brownish clay sand with an average thickness of 2.9m with resistivity ranges of 20-557 ohm-m. The weathered basement underlies the top soil with an average thickness of 26.6m; resistivity ranges between 100-978ohm-m and composed of laterite and clay. This (the weathered and top soil) layers constitute the overburden with an average thickness of 29.5m revealed by the geoelectric section. This weathered basement is a good aquifer in the study area. The depth of probing which is 29.8m is above the depth to the fresh basement

TABLE OF CONTENTS

Title

Page……i

Declaration……ii

Dedication……iii

Certification……iv

Acknowledgement……v

Abstract……vi

Table of Contents……vii

List of Tables……xii

List of Figures……xii

CHAPTER ONE

INTRODUCTION

1.1 General statement……1

1.2 Traditional resistivity survey……2

1.3 Survey Area……3

1.4 Location and Accessibility of the study area……3

1.5 Climate and Vegetation……5

1.6 Statement of the problem……..5

1.7 Justification of the Research……5

1.8 Aims and Objectives……6

1.9 Research Methodology……6

1.10 Review of previous study……6

1.11 Limitation of the research……..7

1.12Choice of the method……8

CHAPTER TWO

GEOLOGY OF THE STUDY AREA

2.1 General geology of the study area……..9

2.2 Geological setting of Zainawa village……9

2.3 Petrology of Zainawa village……..12

2.3.1 Older metasediments……..12

2.3.2 Younger metasediments……12

2.3.3 Older Granites……...12

2.3.4 Younger Granite……13

2.3.5 The Gnesis……..13

2.3.6 Schist……..13

2.4 Basement……13

2.5 Hydrogeology……14

2.6 The weathered basement……14

2.7 The laterite deposit……..15

2.8 The Alluvial deposit…….15

CHAPTER THREE

PRINCIPLES AND THEORY OF THE METHOD USED

3.1 Introduction……16

3.2 Resistivity methods……16

3.3 Resistivity of rocks/mineral……17

3.4 Factor affecting Electrical resistivity of Earth material…….19

3.4.1 Water salinity……19

3.4.2 Porosity of rock……19

3.4.3 Effects of Temperature……20

3.4.4 Effects of rock texture and porosity……20

3.4.5 Effects of Geological process……21

3.5 The theory of the Resistivity method……21

3.6 Single point current electrode at Earths surface……24

3.7 Two point current electrode at Earths surface……..24

3.8 Apparent resistivity……26

3.9 Electrode layout……..26

3.9.1 Symmetrical Schlumberger electrode configuration……..26

3.9.2 Wenner electrode configuration.……...28

3.9.3 Dipole- Dipole layout……..29

CHAPTER FOUR

METHODOLOGY AND FIELD PROCEDURE

4.1 Field procedures and data collection……..30

4.2 The vertical Electric Sounding……..30

4.3 Horizontal Electrical Profiling……...30

4.4 Field Equipment…….....30

4.5 Data collection……..31

4.5.1 Vertical electrical sounding data collection……..31

CHAPTER FIVE

FIELD RESULT AND INTERPRETATION

5.1 Result and interpretation……34

5.2 Interpretation of Resistivity data……34

5.3 Ipi2win Overview……35

5.4 Vertical Electrical Sounding Interpretation……..38

5.5 Electrical Resistivity Sounding……38

5.6 Geoelectric sections along profiles……41 5.6.1 Profile A-B……41

5.6.2 ProfileC-D……42 5.6.3 Profile E-F……43

5.6.4 Profile G-H……44

5.6.5 Profile I-J……45

5.7 Overburden Resistivity Contour map……46

5.8 Aquifer thickness Contour map……47

5.9 Depth to basement……48

5.10 Thickness of overburden……48

CHAPTER SIX

SUMMARY OF RESULTS, CONCLUSIONS AND RECOMMENDATIONS

6.1Summary……52

6.2 Conclusions……53

6.3 Recommendations……53

References……55

Appendix I……59

Appendix II……74

Appendix III……89

LIST OF FIGURES

Figure Title **Page**

1.1 Schlumberger array……1

1.2 Map of Zainawa Village……..4

2.1 Geological map of Nigeria……..11

3.1 A point current electrode on the earths surface……..24

3.2 Two point current electrode on the earths surface……25

3.3 The general four-electrode configuration……..26

3.4 The Schlumberger array……..27

3.5 The wenner electrode configuration……28

3.4 The schematic diagram of Dipole-Dipole array……29

4.1 The Schlumberger arrangement on the field……33

5.1 A simple window for data input……36

5.2 An interface for data model creation and alteration……37

5.3 An interface for viewing, saving and printing result……38

5.4 A digitize curves……39

5.5 Geoelectric section showing profile A-B……42

5.6 Geoelectric section showing profile C-D……43

5.7 Goelectric section showing profile E-F……44

5.8 Goelectric section showing profile G-H……45

5.9 Goelectric section showing profile I-J……46

5.10 Map of resistivity of overburden……47

5.11 Overburden thickness map of the area……49

5.12 Geological Well-Log obtained from National Water Institute…….. ….50

5.13 Geophysical Well-Log obtained from Tahir Company……51

LIST OF TABLES

Table **Title** **Page**

3.1 Resistivities of common rocks/material

And selected ore mineral……18

4-1 Data of VES point A1……..38

Chapter One
Introduction

1.1 General statement

The purpose of electrical survey is to determine the subsurface resistivity distribution by making measurements on the ground surface. From these measurements, the true resistivity of the subsurface can be estimated. The ground resistivity is related to various geological parameters such as mineral and fluid contents, porosity and degree of water saturation in the rock. Electrical resistivity surveys have been used for many decades in hydro geological, mining and geotechnical investigations. More recently, it has been used for environmental surveys. The resistivity measurements are normally made by injecting current into the ground through two current electrodes (C1 and C2 in Figure 1), and measuring the resulting voltage difference at two potential electrodes (P1 and P2). From the current (I) and voltage (V) values, an apparent resistivity (*pa*) value is calculated. $\rho a = K\,V/I$ where *K* is the geometric factor which depends on the arrangement of the four electrodes.

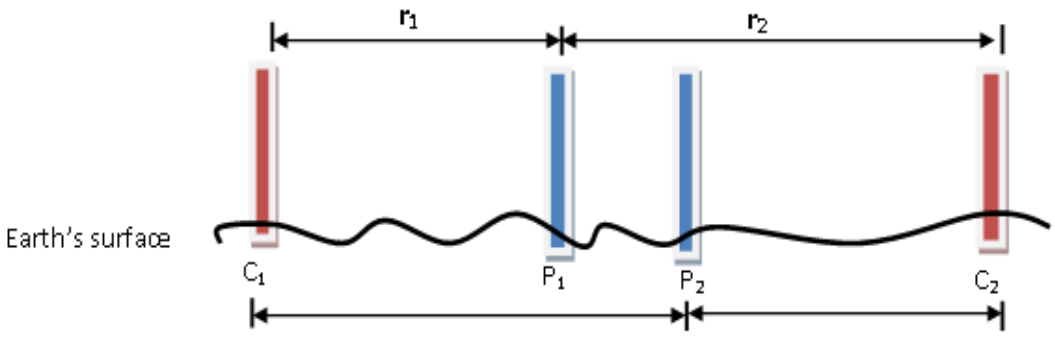


Fig 1.1 Schlumberger array

Resistivity meters normally give a resistance value, R = V/I, so in practice the apparent resistivity value is calculated by $\rho a = KR$

The calculated resistivity value is not the true resistivity of the subsurface, but an "apparent" value which is the resistivity of a homogeneous ground which will give the same electrode arrangement. To determine the true subsurface resistivity, an inversion of the measured apparent resistivity values using a computer programme must be carried out.

1.2 Traditional resistivity surveys

The Resistivity Method has its origin in the 1920's due to the work of the Schlumberger brothers. For approximately the next 60 years, quantitative interpretation, conventional sounding surveys (Koefoed, 1979) were normally used. In this method, the centre point of the electrode array remains fixed, but the spacing between the electrodes is increased symmetrically to obtain more information about the deeper sections of the subsurface.

Figure 1.1 Shows a conventional four electrode array to measure the subsurface resistivity. The measured apparent resistivity values are normally plotted on a log-log graph paper. The data from such a survey were interpret, it is normally assumed that the subsurface of the earth consist of horizontal layers. In this case, the subsurface resistivity changes only with depth, but does not change in the horizontal direction. A one-dimensional model of the subsurface is used to interpret the measurements . Figure 5.2 shows an example of the data from a sounding survey and a possible interpretation model. Despite this limitation, this method has given useful results for geological situations (such as the water-table) where the one dimensional model is approximately true. Another classical survey technique is the resistvity profiling method. In this case, the spacing between the electrodes remains fixed, but the entire array is moved along a straight line. This gives some information about lateral changes in the subsurface resistivity, but it cannot detect vertical changes in the resistivity. Interpretation of data from profiling surveys is mainly qualitative. The most severe limitation of the resistivity sounding method is that horizontal (or lateral) changes in the subsurface resistivity are commonly found. Lateral changes in the subsurface resistivity will cause changes in the apparent resistivity values which might be, and frequently are, misinterpreted as changes with depth in the subsurface resistivity.

In many engineering and environmental studies, the subsurface geology is very complex where the resistivity can change rapidly over short distances. The resistivity sounding method cannot be sufficiently accurate for such situations.

Despite its obvious limitations, there are two main reasons why 1-D resistivity sounding surveys are common. The first reason is the lack of proper field equipment to carry out the more data intensive 2-D and 3-D surveys. The second reason is the lack of practical computer interpretation tools to handle the more complex 2-D and 3-D models. However, 2-D and even 3-D electrical surveys are now practical commercial techniques with the relatively recent development of multi-electrode resistivity surveying instruments (Griffiths et al.,1990) and fast computer inversion software(Loke, 1994).

1.3 Survey Area

Zainawa village via Jogana is situated within the northern Nigeria Basement Complex, in the North, (figure 1.2). With the help of global position system(G.P.S.) the mean altitude of the area is about 600m above mean sea level. The study area (ZAINAWA), where the survey is carried out is bounded by latitude12°36□ to latitude 12° 46□North and longitude 08°26□ to longitude 08°65□East with an average elevation of 600m above sea level.

1.4 Location and Accessibility of the Study Area

Zainawa village via Jogana is situated in Gazewa Local Government Area of Kano state 18km south east of Jigawa state. Accessibility to the Zainawa village is only by the Kano-Jigawa road which is a prominent federal road. A number of all season motorable roads, some of which are old tarred roads also exist within the village.

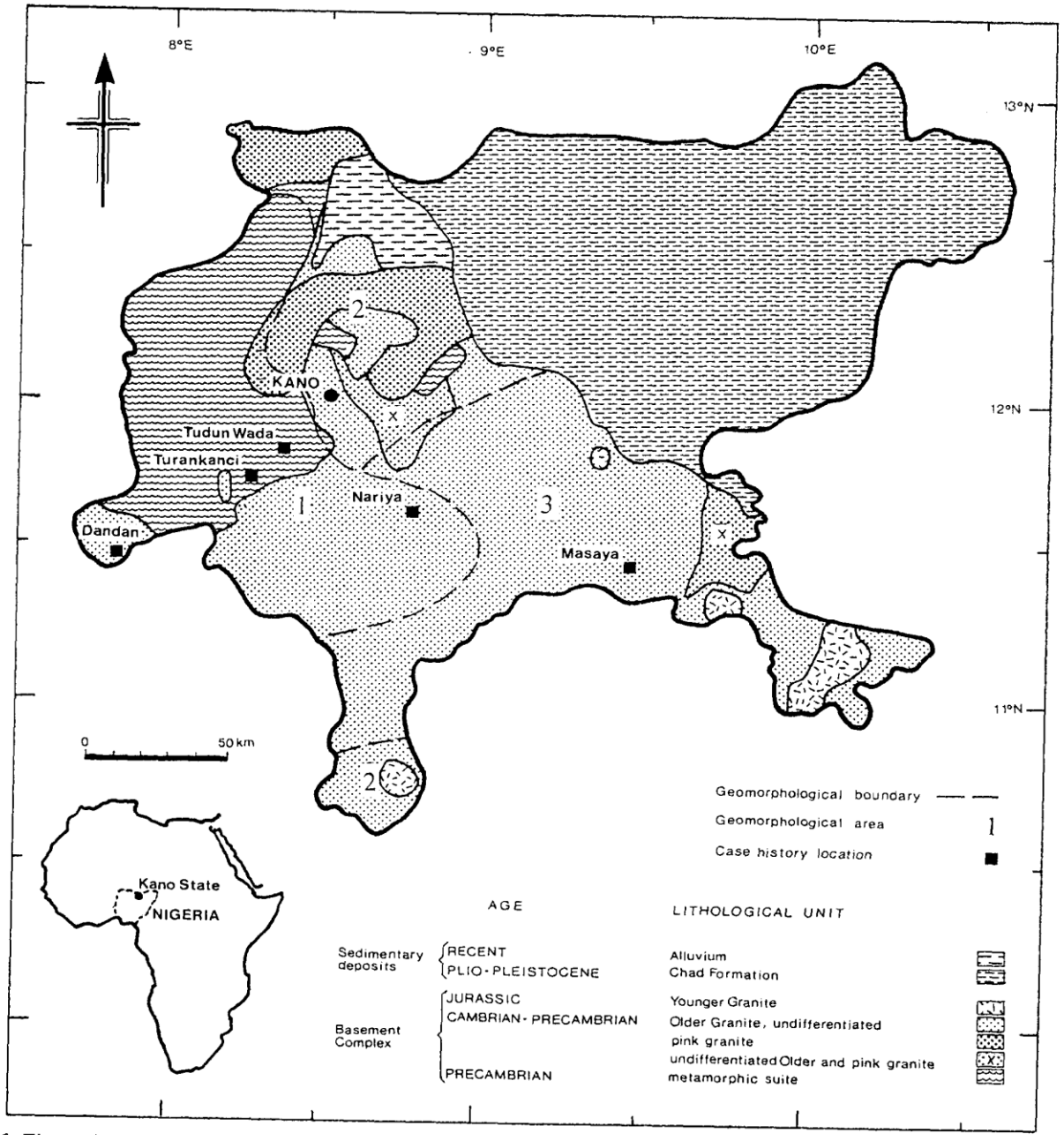


Figure 1.2 Generalized geological map of Kano and Jigawa State (after Jones and Sarah, 1988)

1.5 Climate and Vegetation

The area is in the Guinea Savannah climate belt of Nigeria with distinct dry and wet seasons. The land surface is covered by vegetation which is typical of the savannah grassland that contains the shrub bushes generally; the height of the bushes is less than 3m high and disturbed or interrupted by large isolated trees.

Normally the thick vegetation cover helps to trap rain water and prevent severe runoff which usually gives rise to gully erosion. Despite the scanty nature of the vegetation , thus allowing erosion, it is still of advantage in arresting the depletion of groundwater and reducing the rate of evapotranspiration.

1.6 Statement of the Problem

The statistics failure of structures such as buildings, dams and bridges throughout the nation increased geometrically (Akintorinwa and Adeusi, 2009). The need to identify and/or investigate the cause of such failure has therefore become very imperative so as to prevent loss of lives, time and properties that always accompany such failure. However, the use of geophysical techniques (electrical resistivity, seismic refraction, electromagnetics and ground penetrating radar) which can provide subsurface information is yet to be fully embraced in civil engineering studies.

This information, which is useful in geotechnical analysis, includes depth to bedrock, structural mapping and subsurface characteristics. Such information can also be applied in pre-foundation studies in the design of civil engineering structure. Hence, this research is quite desirable.

1.7 Justification of the Research

The Zainawa village is situated close to the federal road that links Jigawa state and Kano state. The major occupation of the inhabitants is farming. The main purpose of siting a water borehole in the study area over the years, has not been met due to continuous scarcity and the demand nature of the water for various purposes. Therefore, there is need to carry out detailed geophysical investigations of the subsurface so as to delineate geological factors/features in order to site a functional borehole and as well proffer a remedy to the existing problem.

1.8Aim and Objectives

This research is aimed at carrying out the 1D Electrical resistivity survey within the area for hydrogeological and other geological features. Using the Campus Geopulse the following objectives will be achieved:

- To Determine the thickness of the overburden within the area.
- To determine the thickness of the weathered basement within the area.
- To find the variation in the lithology, their thickness and resistivity in the Zainawa village terrain.
- To determine the geoelectrical and hydrogeological characteristics of the aquifers present in the terrain.

1.9 Research Methodology

This research studies, an electrical geophysical method involving the Schlumberger Vertical Electrical Sounding (VES), covering an area of 300.0km^2.This method was used to identify the different geologic factors of Zainawa subsurface. The Schlumberger electrode configuration was used in carrying out the Vertical Electrical Sounding at a separation of 70 metres. A five profile with a total number of 30 VES stations was established on the study area. Each profile at a separation of one hundred meters was taken on the study area. The data collected from Vertical Electrical Soundings were processed using *IPI2Win* (software for interpreting Vertical Electrical Sounding) and the result was used to generate a geoelectric sections.

1.10 Review of Previous Study

In the present study area (Zainawa village), no geophysical work has been done previously. Therefore the present research is meant to provide some geophysical information about the subsurface structure of the place.

Oseji (2002) carried out Vertical Electrical Soundings using schlumberger array to obtain the thickness and depth to the acquifer in Ndokwa village, Delta state.

Esse *et al*.(2011) carried out the application of Electrical Resistivity Technique to evaluate the groundwater potential and aquifer protective capacity at Oru-Imupe, Ogun state, Nigeria, using Schlumberger electrode array, to obtain the resistivity of the weathered basement layers, ranging from 88.6 to 251.1ohm-m and the depth to potential aquifer range from 5 to over 20m.

Louise.(2002), made use of Electrical and Electromagnetic method as a powerful tool in environmental and geotechnical investigations. A technique developed for deeper applications, such as mining, geothermal and crustal studies. However similar work carried out by Water Resources Engineering Agricultural Company (WRECA) on a regional scale that produced a regional geological cross section confirmed the presence of an interface from between the basement complex and sedimentary formations.

Ososami, (1968) carried out vertical electrical sounding to investigate ground water potential in areas around Ahmadu Bello University main campus, Samaru. He revealed in his work that the depth to aquifer in the area varied from about 1m to about 30m. He however, could not clearly demarcate the boundary between the weathered basement and the fresh basement.

Imaging in a confined area (Lokoja New General Hospital in Kogi State) using refraction tomography, showed that seismic refraction tomography probes deeper than geoelectric tomography at the same spread length. That ascertains the fact that seismic method has high accuracy and great penetration. Telford *et al*.(1976).

Farouq. (2007), showed from his geoelectric investigation of the groundwater potential in the Institute for Agricultural Research farm Samaru that the thickness at weathered basement around the area varied from about 3.4m to 30.4m.

1.11 Limitations of the Research

This research covered only about 300.0km^2 of the study area due to logistic and financial limitations. However, within the study area some of the limitations are:

- The frequent disturbance of the local people slowed down the survey being carried out in the study area. This could not be avoided as the local people were the major inhabitants that own and farm on the study area.

- Presence of company wastage and abandoned machine/vehicle along the profile lines.

However, since some of these limitations cannot be overcome at the time of this survey, necessary precautions were applied to minimize them and obtain free and uninterrupted accurate results.

The researcher meet with the village chief and the youth of the village, to draw out some understanding between the inhabitants and the researcher, in order to avoid the frequent disturbance by the farmer.

Also there was an arrangement between the Divisional Police Office in Zainawa Village and the Researcher, in order to avoid any suspicion due to the problem of insecurity in the country at the time of survey.

1.12 Choice of the Method

It is a general expectation that in-fill sediments or fractured rock show a low resistivity contrast with basement crystalline rock and structures, such as dikes, lava dooms. This low resistivity contrast is considered to be a good target for electrical methods. The electrical resistivity 1D survey is a cost effective method, an environmentally friendly; it has the advantage of rapid data collection and interpretation of results than other geophysical methods.

Chapter Two

Geological Setting

2.1 General Geology of the Study Area

Nigeria lies in the Pan African mobile belt which has been affected by Pan-African events through the ages of orogenic, epeirogenic, tectonic and metamorphic cycles. The geology of Nigeria is classified into two parts, the basement complex and the sedimentary basins.The Zainawa village via Gogana in Gazewa Local Government Area of Kano State, lies on a plain which forms part of the vast gentle undulating plain scenery which extends almost unbroken from Jigawa state 18km south east of Kano State. The soil is ferruginous with clay (Kaolinite) and some weathered rocks present (Joda, 1990).

The study area is part of the Nigerian basement complex underlain by crystalline rocks. So, the geology of the area is the same as that of the Nigerian Basement Complex. The rock of the Basement Complex occupies more than 50% of the total land surface of Nigeria, and accommodates the metasediments which are made up of gneisses. Exposure is scanty and highly weathered and decomposed. The rock types are biotites, gneisses, granite gneisses and in parts with subordinate migmatites. The contact between the gneisses and metasediments are gradation.(Mercury,1970).

2.2 Geological Setting of Zainawa Village

Zainawa village is underlain by basement rocks of Precambrian age. They are mainly granites, gneisses and schist (fig.2.0). The Gazewa crystalline rocks are part of the Nigeria Basement Complex. Oyewoye (1964) shows that there is structural relationship between this Basement Complex and the rest of the West African Basement. This is partly due to the fact that the whole region was involved in a single set of orogenic episode, the Pan African orogeny, which left an imprint of structural similarity upon the rock units.

The thrusting imposed on the Basement Complex during the Pan-African orogeny movement is believed to have brought together rocks of different ages with different structural and metamorphic styles (Grant, 1969). The metasediment probably belongs to the sedimentary and granite facies that were formed in a geosynclinals trough which had earlier developed at the end of the Pan African Orogeny (Tokarski, 1972). During the Pan African orogeny, the sediments and igneous material, together with the former metamorphosed rocks became assimilated into the granite intrusions that accompanied the last Orogeny (Grant, 1969).

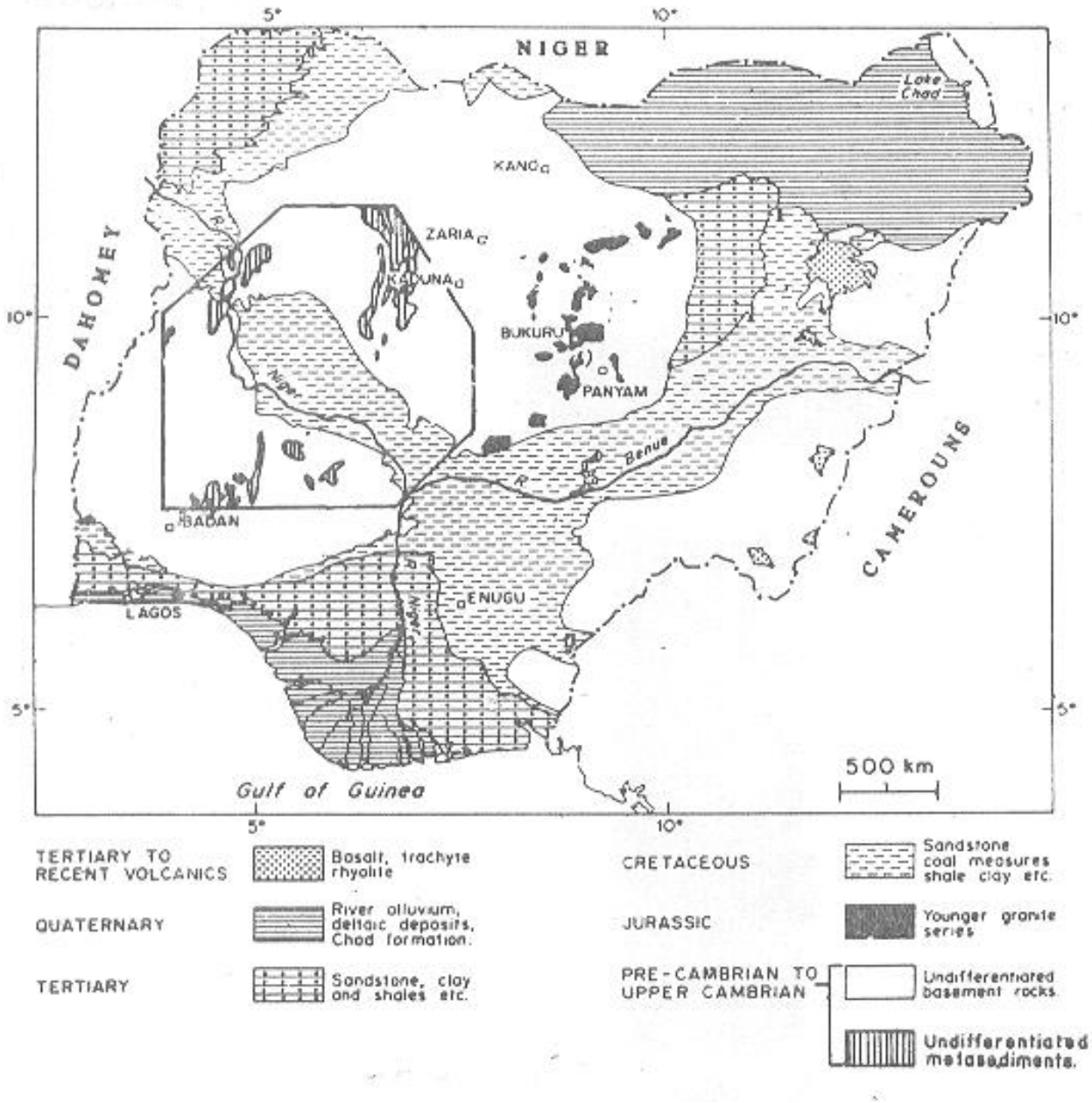


Figure2.1 A generalized geological map of Nigeria (after Kogbe, 1989)

2.3 Petrology of Zainawa Village

The rock types found in Zainawa Village are discussed below:

2.3.1 Older Metasediments

These rocks are believed to be Birrimian (>100 million year) in age and rock types include gneisses which have suffered at least two episodes of tectno-matamorphic deformation resulting in widespread occurrences of migmatitic and granitic gneisses (McCurry, 1976). They occupy isoclinal belts within the crystalline rocks with a N-S trending. Hence, it is overlain by igneous and metamorphic rocks.

2.3.2 Younger Metasediments

The younger metasediments are found in a well defined belt around the north- west and south-west of Nigeria. They are Katanga in age and believed to have been deposited on the originally granitic basement around 1800 million years ago. They were then folded during the Pan-African thermo tectonic events. They occurred as gold bearing quartzites in Ilorin.

2.3.3 Older Granites

They are believed to have intruded the Nigerian Basement Complex during the Eburnean and lower Cambrian ages. The Eburnean granites are fine grained granites that represent a group of minor discordant intrusions of small aerial extent, occurring as dykes and irregular bodies.

The group includes biotite and muscovite granite and adamebites. They are pale brown equigranular and usually foliated. According to Ogunmola *et al*.(2008), the Older Granite Series include rocks intruded during the Pan-African orogenic cycle. The earliest rocks appear to be basic and intermediate intrusives represented by small, irregular bodies of quartz and pyroxene diorite and gabbro. Granitisation on an extensive scale profoundly modified earlier rocks and resulted in widespread migmatites and granitic rocks. This granitisation culminated in the intrusion of a diverse and widespread suite of syn-to late-tectonic granites, granodiorites and syenites. Older granite rocks occur intricately associated with the Migmatite-Gneiss Complex and the Schist Belt into which they generally intruded (Obaje. 2009). They therefore, occur in

most places where rocks of the Migmatite-Gneiss or of the Schist Belt occur. They are found around Wusasa (Zaria), Abuja, Bauchi, Akwanga, Ado-Ekiti and Obudu area.

2.3.4 The Younger Granite

The Younger Granite series or ring complexes that occurred during the time of Mesozoic (Jurassic) are faund in Northern Nigeria to have intruded the Precambrian basement rock. They are confined to zone stretching north-south of the Jos plateau and extend to the Niger Republic with their ages progressively decreasing from Niger Republic towards Nigeria with the youngest rocks found at the southern end of the ring complex. The major tectonic event that took place in the Jos plateau around the Jurassic period resulted in the emplacement of the younger granites and associated rocks assemblage(Grant,1969) outcrop occur as large masses and sometimes as ring dyke. Member include rhyolite, gabbros and syenites.

2.3.5 The Gnesis

The gneissic complex is a medium to coarse grain and are moderate weak foliated rocks. The rocks principally composed of quartz, oligoclase, biotite and occasionally porphyroblastic microcline (McCurry,1970). The older granites are non porphyroblastic and are variably foliated. They contain concordant biotite-rich segregation and are mainly composed of accessory apatite, turbide oligoclase and quartz (Truswell and Cope,1963).

2.3.6 Schist

The schist is found as parallel lenses in the biotitic gneiss. The schist occurs in thin vertical sheets striking in the north-south direction. The schistose metasediment contains mainly biotite feldspar and quartz (Adamu, 1973).Quartzites are often associated and concordant with the schistose lenses.

2.4 Basement

Basement geology was affected by an orogeny which predated the emplacement of the older granite. At the time of this event, the deformation of the basement produced north-south trending basin of metasediment in the form of synclinoria (Truswell and Cope, 1963). Tertiary east

movement tilted the metasediments to the north and warped the basement along the axis of uplift (Russ, 1957). Crystalline rocks of the basement complex may be altered, jointed or fractured. The process of alteration may give rise to loose aggregates above fresh basement or it may create a laterite cover and a clay horizon above loose altered bedrock. Primary porosities of fresh basement rocks are very low and most times less than 30% (Russ, 1957). The rocks have very low permeability due to the presence of a few pores that are interconnected. The weathered profile covering the fresh fractured basement rocks consist of clay and laterite material, the profile changes down to fresh bedrock. This material forms the aquifer.

2.5 Hydrogeology

Hydrogeology is often influenced by the climate, structure and geology of an area. This is because the geological formations underlying the area and their structures determine the type of aquifer to be encountered and the means of recharging them. Some rocks have a dry pore-spaces and others have wet pore-spaces filled with water. The climate determines the water content and the rate of recharge of an aquifer. The climate and hydrological conditions control the surface and subsurface water in the area. The surface water is controlled by the underlying geology, infiltration; evaporation and run off are the major factors responsible for groundwater recharge and accumulation (Umar, 2001). Rainfall is the dominant factor that determines the occurrence of groundwater in the survey area. During the raining season, Zainawa village enjoyed fairly high amount of rain fall. Rain fall data for the last 40 years show that the highest rainfall occurred in the month of August while the lowest is in November.

However, the water table falls progressively through out the dry season. The location of the well from the river is used to determine the amount of water table fall (Olowu, 1967). So the closer a well to the river channel, the smaller the fall. This fall is mainly controlled by subsurface percolation of water into larger river channels. Since the ground is unconfined, there are seasonal fluctuation in the water table (Olowu, 1967).

2.6 The weathered basement

Generally in this region, this is the most important aquifer. The thickness of this aquifer varies from place to place in the area and is covered in most places by lateritic loam (Wrights, 1970, Eigbefo, 1978). Where the weathered basement is exposed to erosion, it exhibits evidence of

mobilization (McCurry, 1970). Where the weathering of the rock has been in situ, which is mostly the case in this area of study, the weathered rocks were capped by laterite.

2.7 The laterite deposit

These deposits contain little water, they are mostly unconsolidated and they are shallow, they receive direct recharge from rainfall. The laterite were found all around the study area. They have varying thickness ranging from less than 1.0m to 10.0m in some places to places of the area, (Wright and McCurry, 1970).

2.8 The alluvial deposit

These consist of gravels, sands, silts and clay deposits. They are mostly found along the river channel and have thickness that vary from 5m-15m (Olowu, 1967).

Chapter Three

Principles and Theory of the Method Used

3.1 Introduction

Geophysical investigations are also employed with engineering objectives in mind, such as predicting the behaviour of earth materials in relation to geological features of subsurface, railways, buildings, tunnels, and nuclear power plants. Surveys are generally identified by the property being measured namely: electrical, gravity, magnetic, seismic, thermal, or radioactive properties. The electric resistivity method was employed in this work to evaluate the integrity of the sub-features beneath the Zainawa village via Jogana in Gazewa L.G.A in Kano State. These methods were used to identify different geologic factors that may affect the enhancement and recharge of water table.

3.2 The Resistivity Methods

The electrical properties of earth materials, consolidated and unconsolidated, vary widely. Various types of unconsolidated materials differ significantly in voids and contain fluids; a consolidated rock, for example sandstone and granite, likewise differ in porosity and fluid content. Their differences affect the conductivity or its reciprocal resistivity. These contrasts between consolidated and unconsolidated materials are usually of a higher order than differences within the two groups; hence electrical exploration for depths of unconsolidated material is generally successful in engineering site investigations.

The general basis of the electric methods of geophysical prospecting is the detection of the surface effect produced by the flow of electrical current inside the earth (Telford *et al*., 1976). In geotechnical branch of civil engineering, the resistivity measurements have been the most widely employed of the electrical subsurface exploration methods.

3.3 Resistivity of Rocks and Minerals

The resistivity of a material is defined as numerically the resistance in ohms between the opposite faces of a uniform unit cube of the material. For a conducting cylinder of resistance *R*, length *l* and cross sectional area *A*, the resistivity is given by

$$\rho = \frac{RA}{l} \qquad (3.1)$$

Electrical resistivity is a physical property of rocks and minerals that shows the greatest variation. Rocks and minerals are considered to be good, intermediate, or poor conductors respectively within the following range;

i. Minerals of resistivity 10^{-8} to about 1 Ωm (mostly metals, graphite, the sulfides etc.)
ii. Minerals and rocks of resistivity 1 to 10^{7}Ωm (most oxides, ores and porous rocks containing water)
iii. Minerals and rocks of resistivity above 10^{7} Ωm (silicates, carbonates, nitrates etc.)

The large contrast in resistivity between orebodies and their host rocks (Table1) is exploited in the electrical resistivity prospecting especially for minerals that occur as good conductors.

Table 1: Resistivities of common rocks/materials and selected ore minerals (Source: Delta Mine Training Centre, Alaska)

Common Rocks/Materials	Resistivity (Ωm)	Ore Materials	Resistivity (Ωm)
Clay	1-100	**Pyrrhotite**	0.001-0.01
Graphitic Schist	10-500	**Galena**	0.001-100
Topsoil	50-100	**Cassiterite**	0.001-10,000
Gravel	100-600	**Chalcopyrite**	0.005-0.1
Weathered Bedrock	100-1000	**Pyrite**	0.01-100
Gabbro	100-500,000	**Magnetite**	0.01-1,000
Sandstone	200-8,000	**Hematite**	0.01-1,000.000
Granite	200-100,000	**Sphaierite**	1000-1,000,000
Basalt	200-100,000		
Limestone	500-10,000		
Slate	500-500,000		
Quartzite	500-800,000		
Greenstone	500-200,000		

3.4 Factors Affecting Electrical Resistivity of Earth Materials

The electrical resistivity of rocks and minerals are extreme variable properties and depend on a number of factors. Bulk resistivities from the surface to more than 15km depth in a normal crust are controlled by aqueous electrolytic conduction by way of pores, fractures, faults, and shear zones. The resistivity of crystalline rock formations such as granulites, granites, and diorites in situ are largely dependent upon the water in the fissures and fractures. Similarly, the porosity, degree of saturation and the nature of pore-electrolytes govern the resistivity of rocks like sandstone and limestone. A slight increase in resistivity with depth is the result of decreasing pore, fracture, fault, and shear-zone porosity due to increased lithostatic load.

3.4.1 Water Salinity

Conduction in near-surface rocks is electrolytic, taking place in connected pore spaces, along grain boundaries, in fractures, faults, and shear zones but negligibly through the silicate framework. The ions which conduct the current result from the dissociation of salts, such dissociation occurr when salts are dissolved in water. Since each ion is able to carry only a definite quantity of charge, it follows that the more ions that are available in a solution, the greater will be the charge that can be carried. Hence, the solution with the larger number of ions will have the higher conductivity. In general, for a given porosity, a rock which contains saline water within its pores will have a greater conductivity when the salinity of the water is high than when it is low. Resistivity decreases with increase in salinity.

3.4.2 Porosity of Rock

Porosity can be defined as the ratio of the percentage of the volume of void space to the total volume of the rock. Porosity arises from the fact that the particles do not occupy all the possible space. It provides a direct measure of the total void space available for the storage of fluids (Clark, 1960)

Resistivity and porosity in sedimentary rocks can be related by the general form of Archie's law, which for rocks devoid of clay is written as

$$f = \frac{\rho_r}{\rho_s} = \alpha\phi^{-m} \qquad (3.2)$$

Where *f* is the formation resistivity factor, ρ_r is the resistivity of the rock, ρ_s is the resistivity of the solution in the pores of the rock, ϕ is porosity, while α and *m* are constants peculiar to the rock type. The constant '*m'* is usually referred to as the *cementation factor* while the constant *α* is referred to as the *coefficient of saturation*. The most common minerals forming soils and rocks have very high resistivity in a dry condition, and the resistivity of soils and rocks is therefore normally a function of the amount and quality of water in pore spaces and fractures. The degree of connection between the cavities is also important.

3.4.3 Effect of Temperature

An increase in temperature lowers the viscosity of water, with the result that ions in the water become more mobile. The increased mobility of the ions results in an observed resistivity decrease with increase in temperature according to the formula (Keller and Frischknecht, 1966)

$$\rho_r = \frac{\rho_{18^\circ}}{1 + \alpha(t - 18^\circ)} \qquad (3.3)$$

Where ρ_r *is* the resistivity at this temperature, *t*, ρ_{18° is the resistivity at 18˚C, α is the temperature coefficient of resistivity (about 0.025/^{o}C for most electrolytes) and *t* is the ambient temperature.

3.4.4 Effects of Rock Texture and Porosity

The texture of a rock dictates its resistivity in the following ways

i. A well sorted sandstone has large void spaces and hence exhibits low resistivity.
ii. A poorly-sorted sandstone will have a much lower porosity and hence will exhibit higher resistivity.
iii. Dissolution along fractures in a limestone will enhance porosity and hence lower resistivity.
iv. Precipitation of some minerals in any rock will lower the porosity and hence increase resistivity

v. Basalt has much unconnected or dead-end pore spaces and hence low permeability, so that even basalt of high porosity may exhibit high resistivity.

3.4.5 Effects of Geological Processes

In general, geological processes reduce the resistivity of a rock but there are exceptions. Weathering of hydrothermal alteration of granite significantly lowers its resistivity. Dissolution, faulting and shearing usually increase porosity and fluid permeability, and hence lower resistivity. Precipitation of calcium carbonate and silica reduces porosity and hence reduce fluid permeability and increase resistivity. Indurations by compaction or metamorphism will reduce porosity and permeability and hence increase resistivity. Salt water intrusion provides more ions for conduction and therefore reduces resistivity.

3.5 The Theory of the Resistivity Methods

The basis of the resistivity method is that when a current is driven into the earth any variation of the surface resistivity will alter the current flow which will in turn affect the distribution of electrical potential (Telford *et al*., 1976).

In the resistivity method, artificially-generated electric currents are introduced into the ground and the resulting potential differences are measured at the surface. Deviations from the pattern of potential difference expected from homogeneous ground provide information on the form and electrical properties of the subsurface inhomogeneities. Generally, the theory used in the resistivity method is derived from Ohm's law which provides the relationship between the magnitudes of the electric field, *E* and current density, *j* and it states that

$$j = \sigma E \qquad (3.4)$$

where σ = conductivity.

Since

$$\sigma = \frac{1}{\rho} \qquad (3.5)$$

where ρ is the resistivity, then

$$j = \frac{E}{\rho} \qquad (3.6)$$

The above definition assumes zero frequency.

For an isotropic medium, the conductivity will be a scalar quantity so that *j* and *E* will be in the same direction. *E* is the gradient of a scalar potential, V in volts. Thus we have

$$E = -\nabla V \qquad (3.7)$$

Hence from equation (3.4) above, we have

$$j = -\sigma \nabla V \qquad (3.8)$$

Taking the divergence of the current density we have

$$\nabla \cdot j = -\nabla \cdot (\sigma \nabla V) = 0 \qquad (3.9)$$

And since σ is a constant equation 3.9 reduces to

$$\nabla^2 V = 0 \qquad (3.10)$$

This is the Laplace's equation, i.e., the potential is harmonic.

For equation (3.10) to hold two boundary conditions must be satisfied;

1. The potential must be continuous across the boundary;

2. The normal component of j must be continuous.

3.6 Single Point Current Electrode at Earth's Surface

Consider a point current electrode C_1 at the surface of the homogeneous isotropic medium and the air above has zero conductivity and the second return current electrode C_2 is at a great distance (Figure 3.1). Equation (3.10) above is then applicable because of symmetry (the potential will be a function of *r* only, where *r* is the distance from the first electrode). The Laplace's equation in spherical coordinates simplifies to equation (3.11)

$$\nabla^2 V = \frac{d^2V}{dr^2} + \left(\frac{2}{r}\right)\frac{dV}{dr} = 0 \qquad (3.11)$$

Multiplying by r^2 and integrating, we get

$$\frac{dV}{dr} = \frac{A}{r^2} \qquad (3.12)$$

Integrating again, we have

$$V = -\frac{A}{r} + B \qquad (3.13)$$

where *A* and *B* are constants. From the above equation $V = 0$ when $r \rightarrow \infty$, we get $B=0$. In addition, all the current flows through a hemispherical surface in the lower medium, thus the total current crossing the hemisphere is given by

$$I = 2\pi r^2 J = -2\pi r^2 \sigma \frac{dV}{dr} = -2\pi\sigma A \qquad (3.14)$$

Hence,

$$A = -\frac{I\rho}{2\pi} \qquad (3.15)$$

And from equation (3.13)

$$V = \frac{I\rho}{2\pi r} \qquad (3.16)$$

or, $\rho = \frac{2\pi r V}{I}$ (3.17)

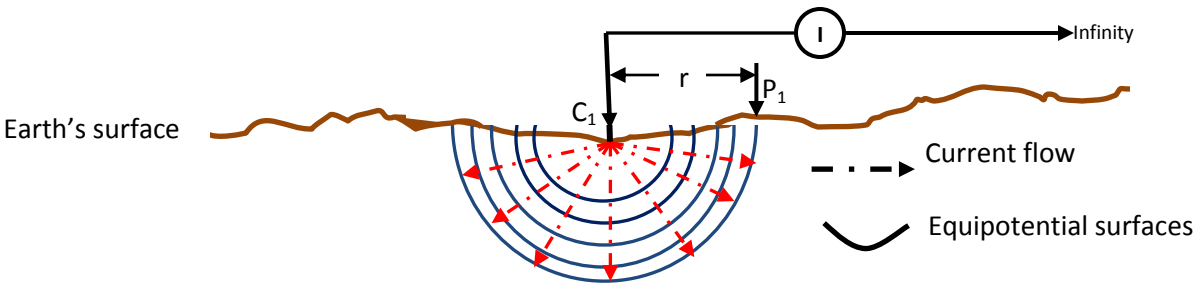


Figure 3.1: A point current electrode on the earth's surface (and the second electrode at infinity).

3.7 Two Point Current Electrodes at Earth's Surface

Consider two point current electrodes in which the distance between them is finite (Figure 3.2). The potential at any near surface point will be affected by both current electrodes and hence the potential due to C_1 at P_1 is

$$V_1 = -\frac{A_1}{r_1} \quad (3.18)$$

And the potential due to C_2 at P_1 is

$$V_2 = -\frac{A_2}{r_2} \quad (3.19)$$

Where $A_1 = -A_2 = A$ thus, we have

$$V_1 + V_2 = \frac{I\rho}{2\pi}\left(\frac{1}{r_1} - \frac{1}{r_2}\right) \quad (3.20)$$

Introducing the second potential electrode at P_2 the potential difference between the two potential electrodes is given by

$$\Delta V = \frac{I\rho}{2\pi}\left\{\left(\frac{1}{r_1} - \frac{1}{r_2}\right) - \left(\frac{1}{r_3} - \frac{1}{r_4}\right)\right\} \quad (3.21)$$

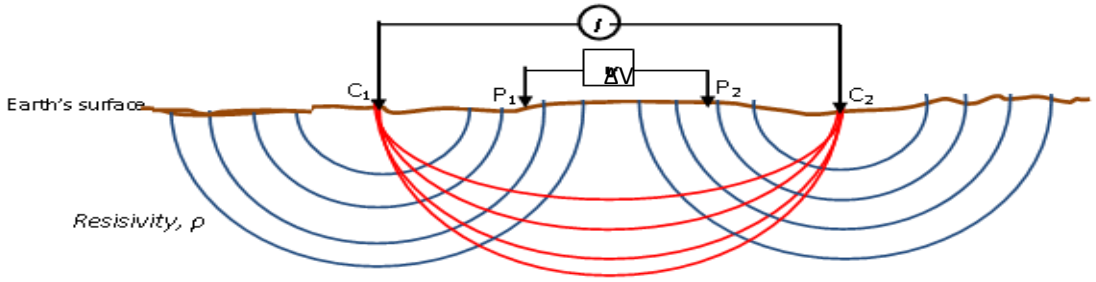


Figure 3.2 Two point current electrodes on the earth's surface (Red line is current flow. Blue line is equipotential surfaces)

Equation (3.21) gives the potential difference between the two potential electrodes. The electrode layout is referred to as the general four-electrode configuration over a homogeneous isotropic earth, a variation of which is normally used in electric resistivity measurements (Figure 3.3).

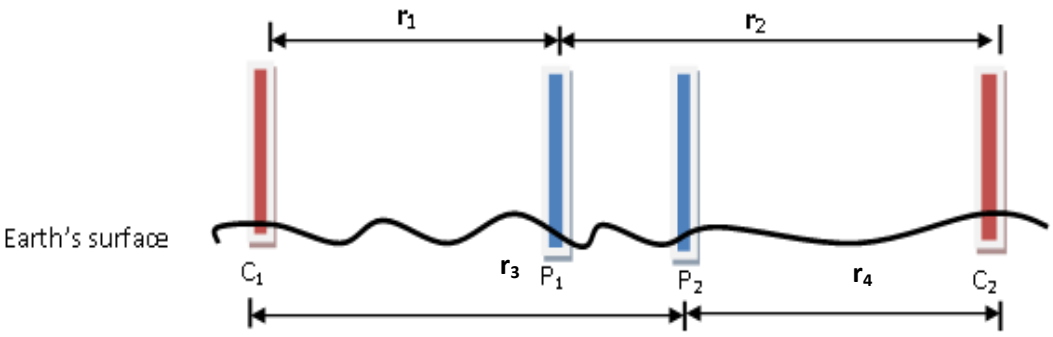


Figure 3.3 The general four-electrode configuration

3.8 Apparent Resistivity

From equation (3.21), the resistivity, ρ is given by

$$\rho = \frac{\Delta v}{I} \frac{2\pi}{\left[\left(\frac{1}{r_1} - \frac{1}{r_2}\right) - \left(\frac{1}{r_3} - \frac{1}{r_4}\right)\right]} \quad (3.22)$$

$$\rho = k \frac{\Delta v}{I}$$

where the parameter k, has to do with the electrode geometry. Wherever these measurements are made over a real heterogeneous earth, as distinguished from the fictitious homogeneous half-space, the symbol ρ is replaced by ρ_a. This measured resistivity is called the *apparent resistivity* since the measured resistivity is usually a composite of the resistivity of several layers.

3.9 Electrode Layouts

The electrical resistivity method uses a series of electrodes nailed to the ground about six inches deep along a straight profile or 3-D grid. The distance between the electrodes depends on the desired depth of investigation and the target to be imaged. The farther apart the electrodes the "deeper" the electricity goes into the earth, at the expense of resolution. This is because the fraction of total current that flow at depth varies with the current-electrode separation. Usually the depth of penetration is about one-third of the current electrode spacing. The most commonly used configuration activates four electrodes at a time, two for passing current into the ground and two for measuring the potential difference; these are the Wenner, the Schlumberger and the dipole-dipole electrode layout.

3.9.1 Symmetrical Schlumberger Electrode Configuration

In this array, the current electrodes are spaced much further apart than the potential electrodes (Figure 3.4). The electric field is measured approximately. Thus from equation (3.22) the apparent resistivity is given as

$$\rho_a = \pi\left(\frac{l^2}{2b} - \frac{b}{2}\right)\frac{\Delta V}{I} \qquad (3.23)$$

where l is the distance of the current electrode from the sounding point and b is the potential electrode distance from the sounding point. In sounding, the potential electrodes are fixed while the current electrode separation is increased symmetrically about the centre of spread.

Schlumberger array are carried out under the constraint that potential electrode spacing (MN) is small compared to the current electrode spacing (AB), i.e. MN <AB/2.

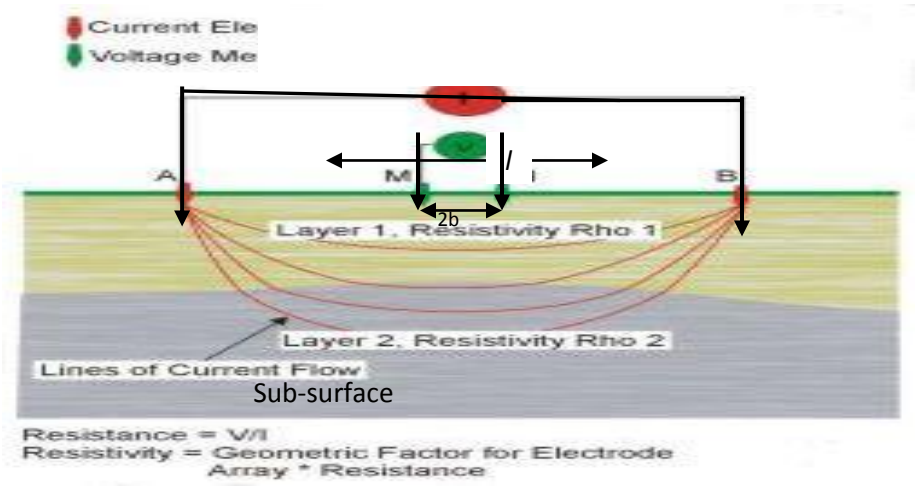


Figure 3.4 The Schlumberger array; A and B are current electrodes, while M and N are potential electrodes.

In this research the Schlumberger electrode configuration was used to carried out the vertical electrical soundings because of the following reasons;

i. The effect of local and shallow inhomogeneities near the electrodes is constant for all measurements since the potential electrodes are kept fixed.

ii. Schlumberger array is faster in field operations, since only the current electrodes must be moved between all readings while the potential electrodes are moved only exceptionally. It is therefore more effective since the array saves time and manpower.

iii. The relative error resulting from the electrode effect is same for all measurement and these can be handled easily.

3.9.2 The Wenner Electrode Configuration

The Wenner Electrode Geometry is illustrated in figure 3.5. Spacing between all electrodes is equal and conventionally denoted by letter '*a*' in conducting the horizontal electrical profiling with this configuration all electrodes are moved along a straight line or profile after every reading such that the spacing between electrodes remains equal and takes on certain preselected values. Typically, one endeavours to achieve values of '*a'* that are equally spaced on a logarithmic scale and ideal number six points per decade (e.g. 10.0, 14.7, 21.5, 31.6, and 46.4) (Burger and Burger, 1992). The general equation for the apparent resistivity in this configuration is given by

$$\rho_a = 2\pi a \frac{\Delta V}{I} \qquad (3.24)$$

The major advantages of this configuration are;

i. The larger potential electrode spacing places less demand on the instrument sensitivity

ii. The simplicity of the apparent resistivity equation (equation 3.22) when the electrodes are equally spaced (equation 3.24).

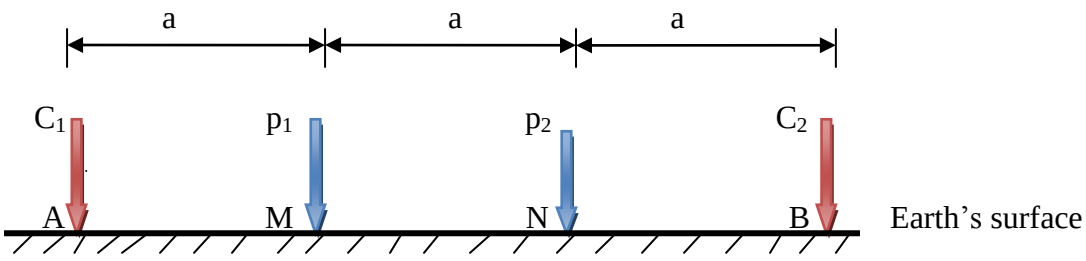


Figure 3.5 A Schematic Diagram of Wenner array

3.9.3 Dipole-dipole layout

This array is widely used in resistivity/IP surveys because of the low Electromagnetic coupling between the current and potential circuit. The spacing between the current electrode pair, C_2-C_1, is given as ”a” which is the same as the distance between the potential electrode pair P_1-P_2. The factor “n” is the ratio of the distance between the C_1 and P_1 electrodes to the C_1-C_2 or P_1-P_2 dipole. Separation “a” for surveys with this array, the “a” spacing is initially kept fixed and the “n” factor is increased from 1to2to3 until up to about 6 in order to increase the depth of investigation.

The dipole-dipole array is very sensitive to horizontal changes in resistivity but relatively insensitive to vertical changes in the resistivity. It is good in mapping vertical structures, such as dykes and cavities, but relatively poor in mapping horizontal structures such as sedimentary layers.

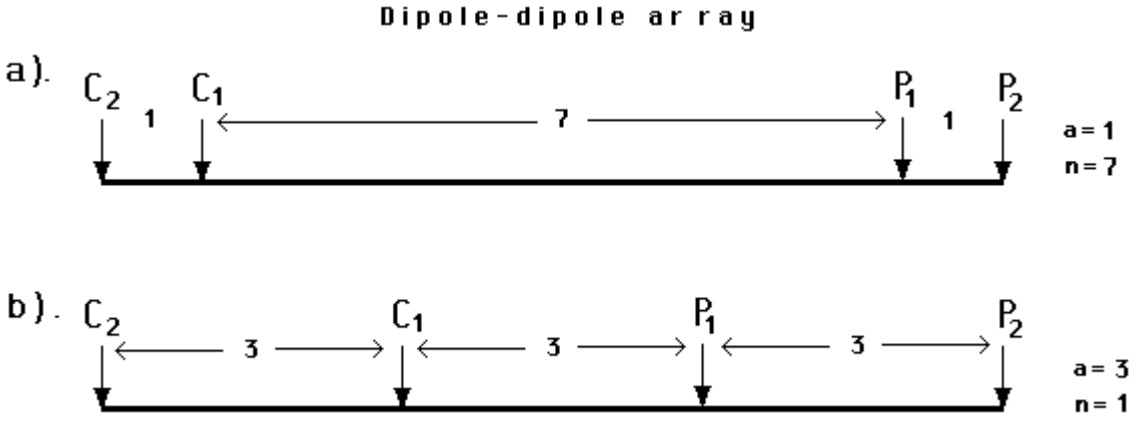


Figure:3.6 The schematic diagram of Dipole-dipole array.

Chapter Four

Methodology and Field Procedure

4.1 Field Procedures and Data Collection

Whichever configuration is used, there are two procedures for carrying out the resistivity field survey depending on whether one is interested in resistivity variations with depth or with lateral extend, and these are the Vertical Electric Soundings.

4.2 The Vertical Electric Sounding

Using the schlumberger configuration, the potential electrodes remain fixed while the current-electrode spacing expands symmetrically about the center of spread. As the current electrodes spacing increased progressively, it may become necessary to increase the potential electrodes spacing in order to obtain a measurable potential. This method is useful in determining depth of overburden, structure and resistivity of flat-lying sedimentary beds and possibly of the basement (Telford *et al*., 1976).

4.3 Horizontal Electrical Profiling

The Wenner Electrode Configuration can be used to carry out the horizontal electrical profiling in other to determine the lateral variations of resistivity along the profile. The current and potential electrodes are maintained at a fixed separation and progressively moved along a profile. This method is widely employed to locate faults or shear zones and to detect localized bodies of anomalous conductivity. It is also used in geotechnical surveys to determine variations in bedrock depth and can also indicate the presence of potentially unstable ground conditions (Kearey *et al.,* 2002).

4.4 Field Equipment

The instrumentation used for this survey consists of the Campus Geopulse Terrameter SAS 300, four steel electrodes, field hammers, measuring tape and reels of wire. The Campus Geopulse

Terrameter SAS 300 measures the resistance and displays it on its screen board depending on its magnitude, it may be in kilo ohms, ohm or milliohms. The Campus Geopulse Terrameter contain three basic sub-units; a microprocessor for monitoring, control and computation; an electrically isolated transmitter for the supply of defined regulated signal current and finally a receiver of voltage, correlated with the transmitted signal current. It can operate at frequency as low as 4 cycles per second; this property makes it suitable for greater depths of investigation. It is portable. It carries out signal averaging by taking consecutive readings automatically and displaying the average result. This makes it possible for the terrameter to extract the signal from any form of noise.

4.5 Data Collection

The resistivity of the subsurface varies vertically with depth and laterally with distance. Both of these variations give useful information about the sub-surface structures. It is therefore necessary to look at these variations. In this case study, the vertical electrical sounding are carried out to investigate the resistivity variation vertically and to determine the depth of the weathered basement.

4.5.1 Vertical electrical sounding data collection

Five profiles, with a total of 30 Vertical Electrical Soundings (VES) and each (VES) was taken on the surface of the area. The station interval between the VES stations along each profile is 100 metres apart. A maximum current electrode spacing (AB) of 200 metres was used with the aim of probing a depth of at least 1/4 of AB (Gholam and Mohammed, 2005).

In this method, a fixed point called the VES station was marked and noted. Two current electrodes C_1 and C_2 of equal distance on the opposite sides of the VES station were measured and driven into the ground with the aid of a sledge hammer for proper contact to be made with the ground. Similarly, two other electrodes called the potential electrodes P_1 and P_2 of equal distance from the sounding point and between the current electrodes were measured and driven into the ground with the aid of the sledge hammer for proper contact to be made also with the ground. The arrangements of the current and potential electrodes were in such a way as to maintain a straight line. These electrodes were connected to the terrameter through their

respective switch (Figure 4.0). The terrameter was switched "ON" and current was introduced artificially into the earth through the pair of electrode C_1 and C_2 and the resulting potential difference due to the current was measured through the other pair of electrode P_1 and P_2. Any subsurface variation in resistivity/conductivity alters the current flow, which in turn affects the distribution of electrical potential at the surface. Thereafter the terrameter was switched "OFF". The field procedure consists of expanding current electrodes (C_1 and C_2) while holding potential electrode's distance (P_1 and P_2) fixed. This process yields a rapidly decreasing potential difference across P_1 and P_2, which ultimately exceeds the measuring capabilities of the instrument. At this point, a new value for potential distance was established, typically five times greater than the preceding value (Keller and Frischknecht, 1966; Osemeikhian and Asokhia, 1994). This systematic movement of the current and potential electrodes continued until the survey was completed. A current variation in the ranged of 0.2-1.0A, found suitable in basement terrain was used during the measurements. (Badmus *et al.*, 2005).

The numerical values of the geometric factors for each pair of the current electrode spacing were determined so that the apparent resistivity was calculated on the field easily.

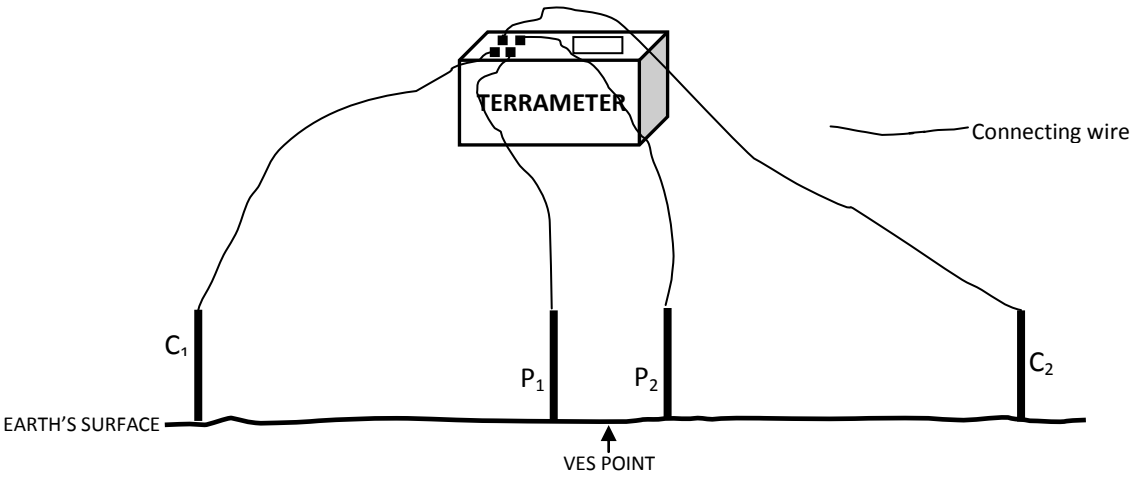


Figure 4.1: The Schlumberger arrangement of the current and potential electrodes as used in the field.

Chapter five

Discussion

5.1 Results and Interpretation

The data analysis for the VES was performed using IPI2Win's new method for the automatic interpretation of schlumberger sounding curves. This method was used to obtain the model for the apparent resistivity of each sounding. The resulting true resistivity layer model from the application is shown in figure 5.1. The true resistivity models at sounding points were used to produce geoelectric section along profiles A-B, C-D, E-F, G-H and I-J Profiles are parallel to each other, this was deliberately chosen to observe and investigate continuity of the subsurface structures.

5.2 Interpretation of Resistivity Data

An exclusively quantitative interpretation of apparent resistivity data is often difficult because of the wide variations in resistivity possessed by geological materials and the difficulty in developing theoretical expressions for apparent resistivity of all but the simplest geometries (Burger and Burger, 1992). There are so many methods of interpreting apparent resistivity data. These are the empirical methods which included Moore Cumulative Resistivity Method (Moore, 1945) and the Barnes Layer Method(Barnes, 1950). Analytical Method, which involves the curve matching, the computer-based etc.

The computer-based approach is suggested by Zohdy (1989). Recently, due to the advancement in modern technology, different computer programmes have been designed to ease the ambiguity in the interpretation of apparent resistivity data. However, because of the problem of equivalence and suppression and because of the many factors that affect curve details, a thorough knowledge of resistivity principles and as much experience as possible must go hand-in-hand with computer-derived solutions for field measurements (Burger and Burger, 1992). In this research *IPI2Win* is used in Vertical Electrical Sounding interpretation.

.

5.3 IPI2Win Overview

IPI2Win is designed for vertical electrical sounding and/or induced polarization data obtained with any of a variety of the most popular arrays used in the electrical prospecting (Bobachev *et al*., 2001). Special attention is paid to the user-friendly interactive interpretation. Due to handy control, the interpreter is able to choose from a set of equivalent solutions, the one best fitting both geophysical data (i.e. providing the least fitting error) and geological data (i.e. geologically sensible resistivity cross-section).

The main important menu in the IPI2Win software include;

- File: this contained controls for opening a new VES point, adding a file, exporting a file, printing curves, reopening existing file etc.
- Edit: this contained controls for copying a file, discarding the latest change of a model, restoring the model sounding point, Dar-Zarrock analysis, synthetic curve analysis etc.
- Point: this contained controls for inversion, profile inversion, new model generation etc.
- Section: this contained controls for zooming in and out, more depth resolution, resistivity section etc.
- Tool: this contained controls for statistical analysis, equivalence and conductance viewing.

The software has the capabilities of data management, curve interpretation and result management. The main interactive features of the software are the data entering, data correction and data alteration.

Entering data: *IPI2Win* internal utility for creating data file is run by choosing the File, New VES point menu item, or by clicking the new VES point button on the toolbar. The new VES point window will appear. The left part of the window is a table of field data, each line represents spacing. The columns of the table are current electrode spacing (AB/2 column), potential electrode spacing (MN), apparent chargeability (SP), voltage (U), current (I), coefficient (K), and apparent resistivity (ohm-m). Current electrode spacing and potential electrode spacing must be typed into the corresponding cells of the table. To enter the voltage and current (in the case where the instrument do not measure the resistivity directly) click the

input U and I button of the window, and then type the values in the corresponding cells. The array type used must be selected from the Array drop-down list of the window. After all the data are entered click "*OK*" button of the window (figure5.1).

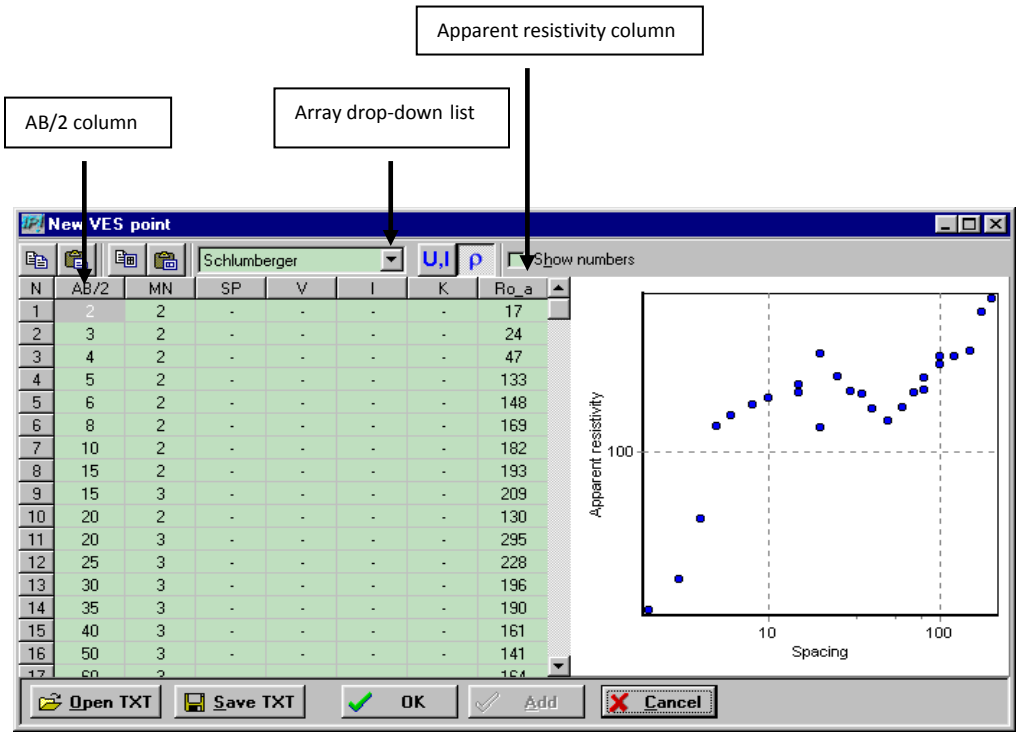
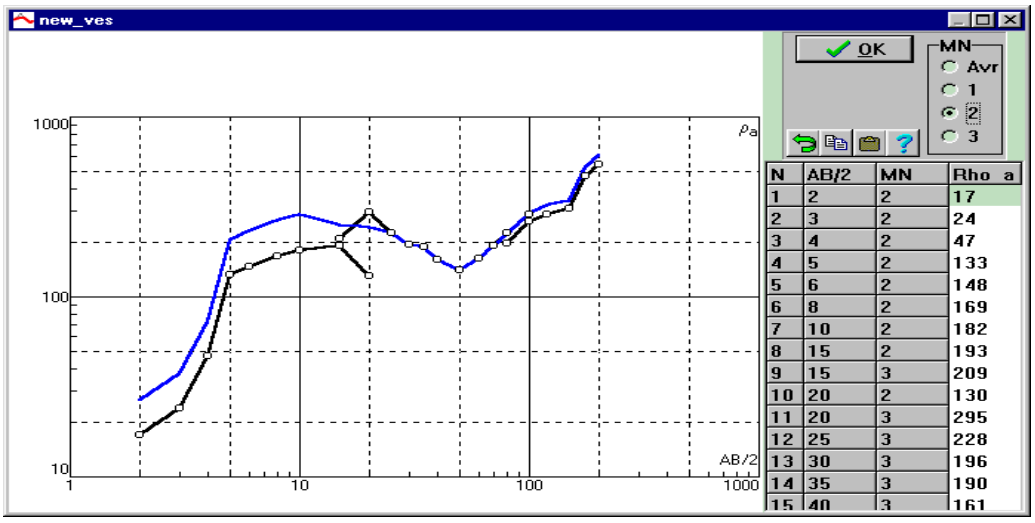


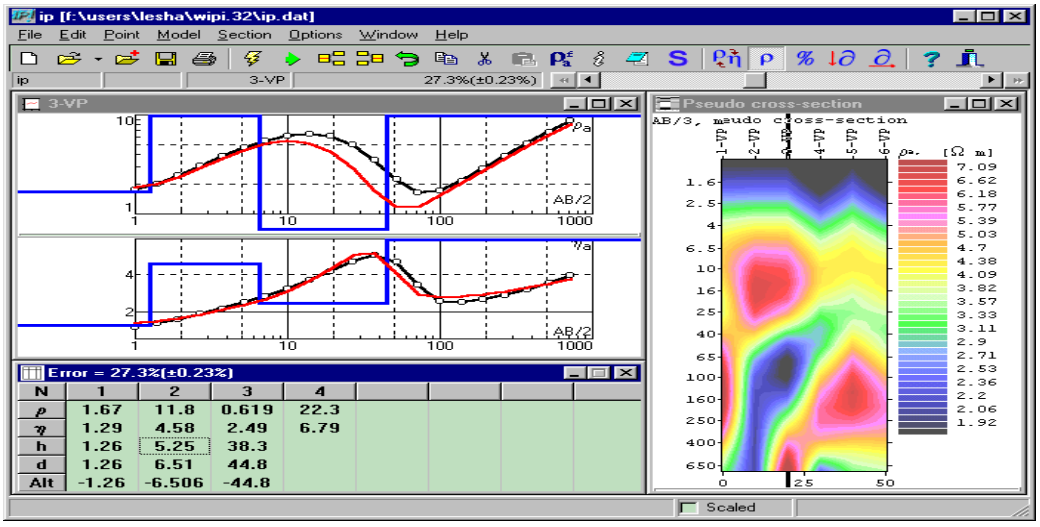
Figure5.1 A simple window for data input

Data correction and alteration: After clicking the OK button of the window, a new window appears displaying the field curve, synthetic curve field model and a table for the field model. The curve is plotted on a logarithmic scale for both axes. This window allowed for data correction and alteration. This is however possible based on the interpreter skills and knowledge of the theory of resistivity (Figure 5.2). After this is carried out the result obtained can be save, copy as bitmap or print out directly (Figure 5.3)



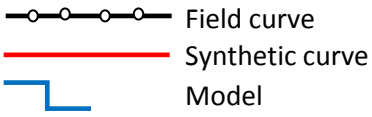
N	AB/2	MN	Rho a
1	2	2	17
2	3	2	24
3	4	2	47
4	5	2	133
5	6	2	148
6	8	2	169
7	10	2	182
8	15	2	193
9	15	3	209
10	20	2	130
11	20	3	295
12	25	3	228
13	30	3	196
14	35	3	190
15	40	3	161

Figure 5.2 An interface for data model creation and alteration



N	1	2	3	4
ρ	1.67	11.8	0.619	22.3
η	1.29	4.58	2.49	6.79
h	1.26	5.25	38.3	
d	1.26	6.51	44.8	
Alt	-1.26	-6.506	-44.8	

Figure 5.3 An interface for viewing, saving and printing result



5**.4 Vertical Electrical Sounding Interpretation**

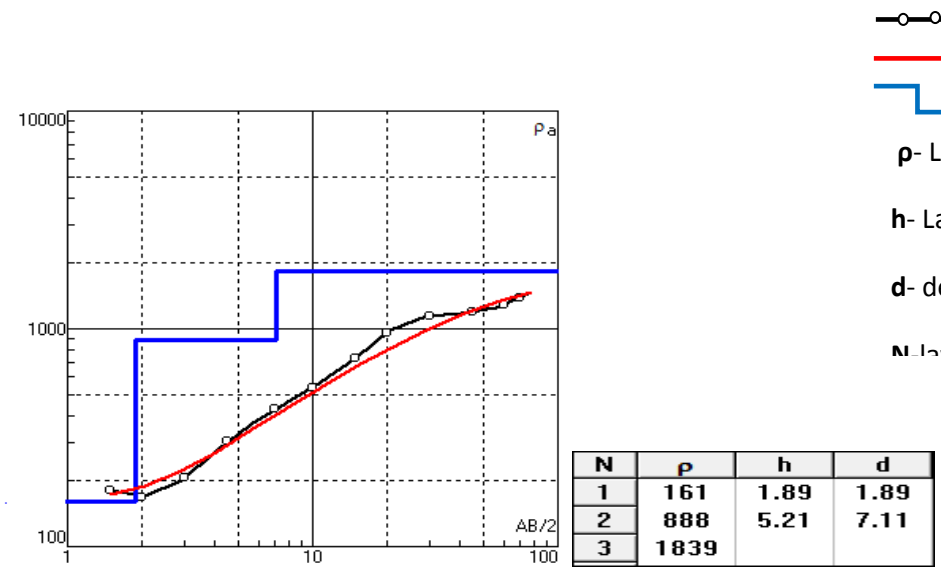
The value of the apparent resistivity at each sounding point was calculated and interpreted using the IPI2Win computer software as it was shown in the appendix II.

5.5 Electrical Resistivity Sounding

Based on the IPI2Win's method, the field curves were found to be averagely four (4) layers. From appendix I, Table A1, A2, A3 ,A4 and A5 show the interpretation of VES POINT A1, A2, A3, A4 and A5 respectively. And figure 5.4a, 5.4b, 5.4c, 5.4d and 5.4e shows the typical digitized curves for VES POINT A1, A2, A3, A4 and A5 respectively.

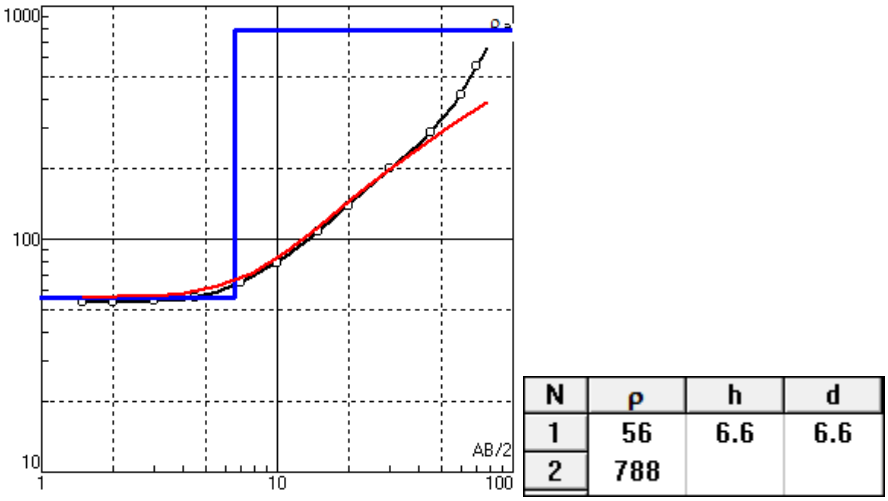
Table 4.1a: Data of VES POINT A1.

AB/2 (m)	MN/2 (m)	K-FACTOR (m)	RES (ohms)	APP RES (ohm-m)
1.5	1.0	1.964	94.2	185
2.0	1.0	4.712	21.7	102
3.0	1.0	12.568	13.2	166
4.5	1.0	30.243	8.6	260
7.0	1.0	75.408	6.6	498
10.0	1.0	155.529	4.1	638
15.0	2.0	173.596	7.1	1233
20.0	2.0	311.058	5.3	1649
30.0	2.0	703.808	2.2	1548
45.0	2.0	1587.496	0.9	1429
60.0	2.0	2824.658	0.5	1412
70.0	2.0	3845.808	0.3	1154



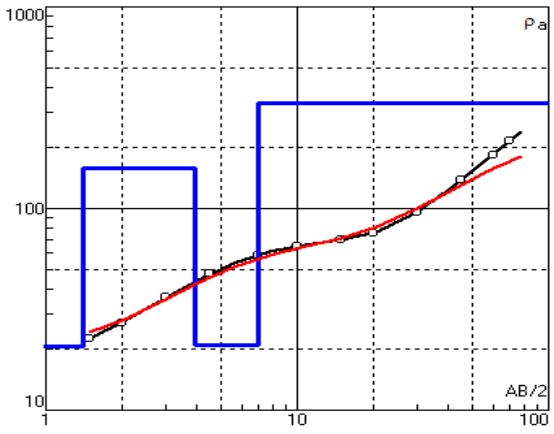
N	ρ	h	d
1	161	1.89	1.89
2	888	5.21	7.11
3	1839		

Fig; 5.4a; The graph of VES point A1



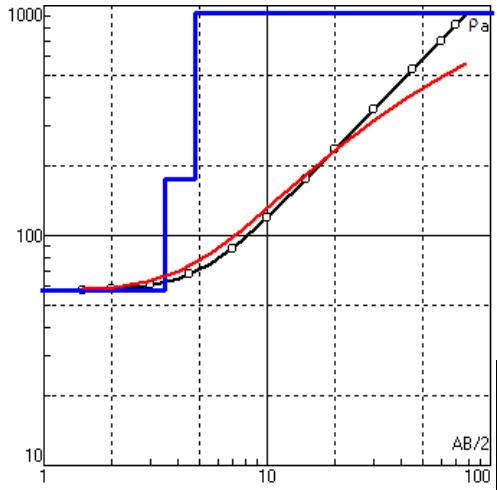
N	ρ	h	d
1	56	6.6	6.6
2	788		

Fig: 5.4b: The graph of VES point A2



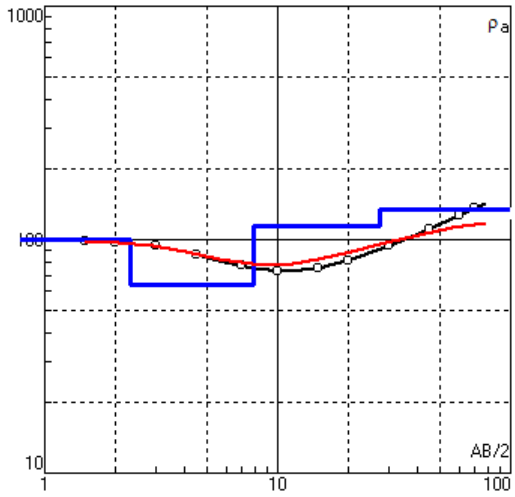
N	ρ	h	d
1	20	1.41	1.41
2	159	2.49	3.89
3	21	3.12	7.01
4	333		

Fig: 5.4c: The graph of VES point A3



N	ρ	h	d
1	57	3.48	3.48
2	175	1.28	4.76
3	928		

Fig: 5.4d: The graph of VES point A4



N	ρ	h	d
1	99	2.33	2.33
2	64	5.55	7.88
3	114	19.6	27.5
4	135		

Fig: 5.4e:The graph of VES point A5

The interpretation of all the VES points (A1 to E6) is shown in Appendix I.

In figure 5.4a, 5.4b, 5.4c, 5.4d and 5.4e, apparent resistivity (ρ_a) in ohm-meters' is plotted against the electrode spacing (AB/2) in meters' by the computer software IPI2Win on a log-log scale. The blue colour gives the number of layers, the red colour indicate the calculated curve while the black colour gives the observed curve for the field data.

5.6 Geoelectric Sections along Profiles

5.6.1 Profile A-B

Figure 5.5 shows the geoelectric section along profile A-B. Four lithological layers are distinguished. The top soil has resistivity ranging from 20-161 ohm-m and with an average thickness of 2.5m. This layer consists of laterite, clay and silt. Underlying the above layer is a formation where the resistivity is between 64-888 ohm-m and average thickness of 9m. This is likely the weathered basement. The third layer has resistivity range of 746-1046 ohm-m and thickness varying from 15 to 35m. This layer is presumably the fractured basement. The last layer of infinite thickness has resistivity greater than 500ohm-m. This is probably the fresh basement.

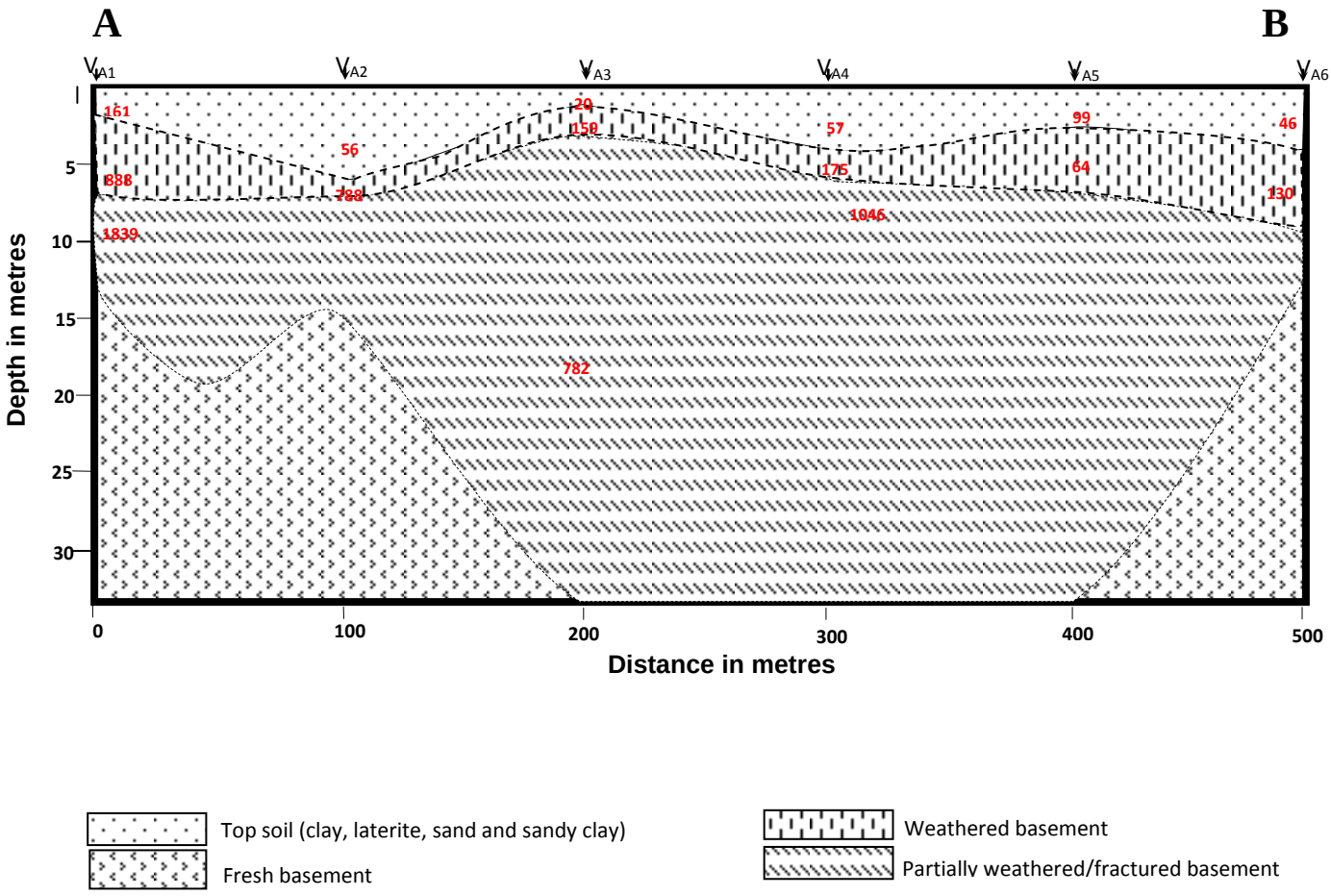


Figure 5.5 A Geoelectric section along profile A-B.

5.5.2 Profile C-D

Geoelectric section along the profile C-D has three subsurface layers (fig. 5.6). The top soil has resistivity value ranging from 81 to192 ohm-m and average thickness of 1.6m. The presence of laterites around VESB5 may be responsible for the low resistivity value. The second layer resistivity varies from 38 to 448 ohm-m and average thickness of 25-30m. The values are low compared to other layers and may be consisting of clay lenses. This layer is presumably the fractured basement. The third layer whose resistivity value is greater than 600ohm-m with infinite thickness is probably the fresh basement.

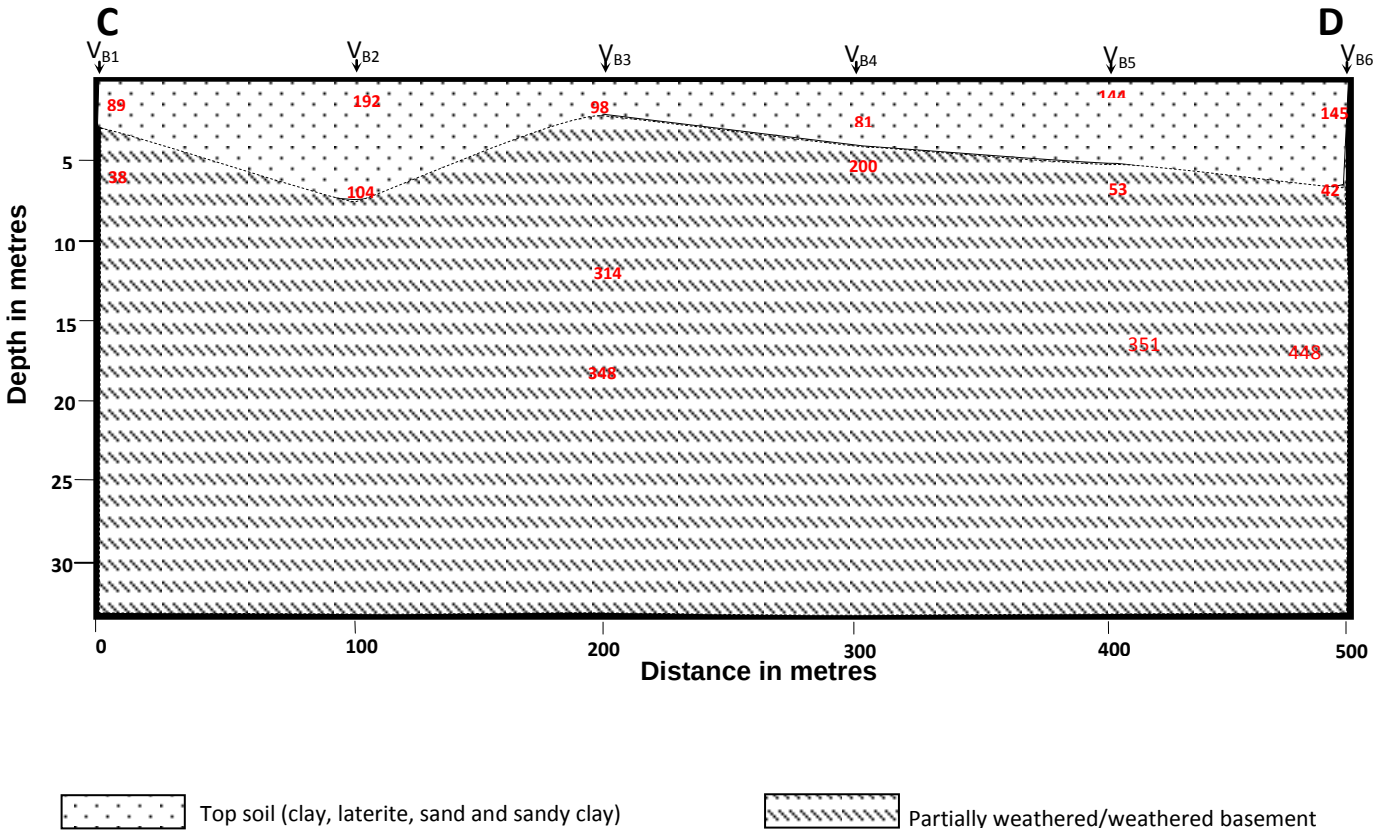


Figure 5.6 Geoelectric section along profile C-D

5.5.3 Profile E-F

The geoelectric section along profile E-F has three layers (Figure5.7). The top soil layer has a resistivity range of 44-170 ohm-m with an average thickness of 3m. The presence of fadama loam around VES C3 may be responsible for the low resistivity value. The second layer resistivity varies from 67-233 ohm-metre with an average thickness of 3.5m. The low resistivity value of this layer indicates the presence of laterite in the area. The third layer has resistivity range of 102-1000 ohm-m with an average thickness of 30m. The resistivity of this layer at VES C3 is low compared to VES C4 and C5. This layer with low resistivity is most likely the most conductive layer under the profile. The fourth layer has resistivity greater than 1000 ohm-m with an infinite thickness and depth.

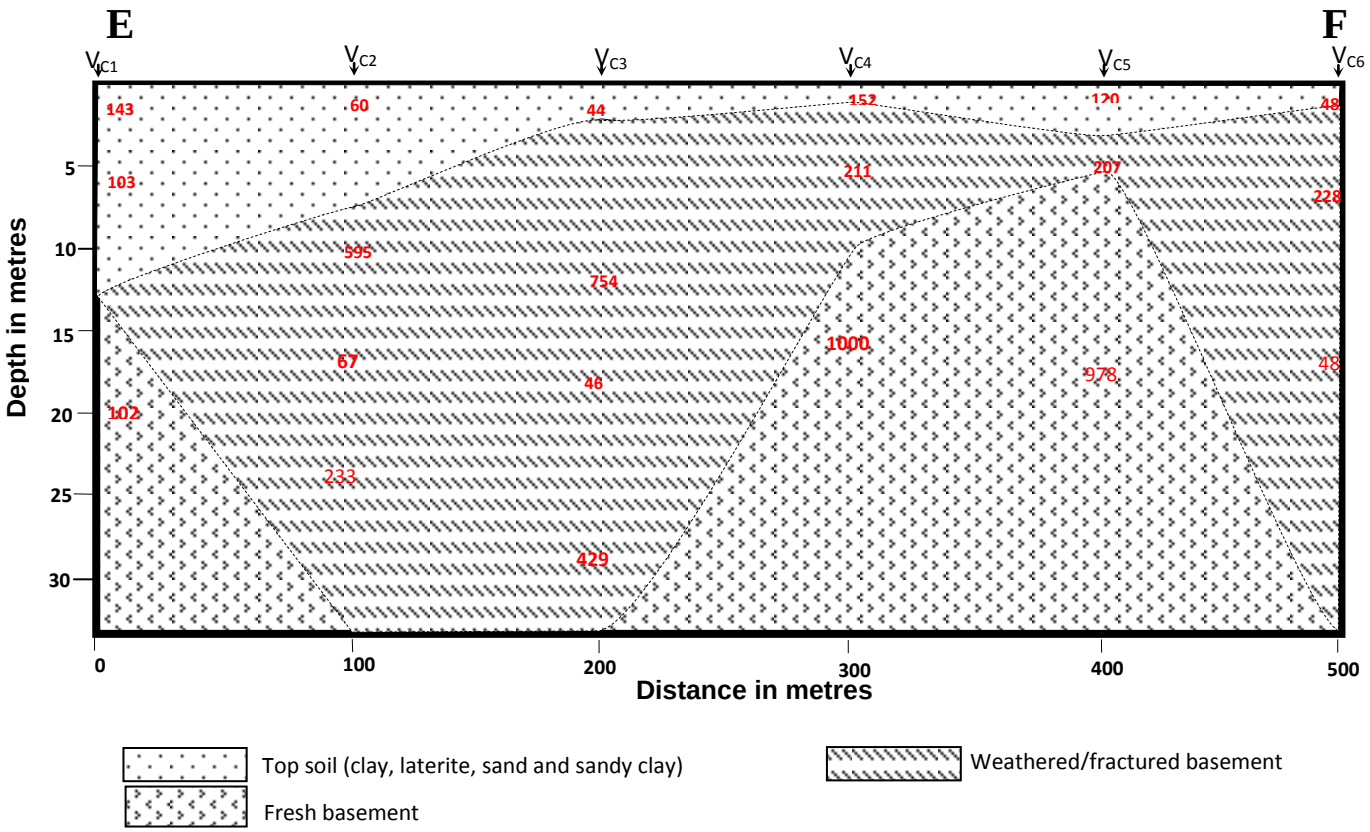


Figure 5.7 Geoelectric section along profile E-F

5.5.4 Profile G-H

Figure 5.8 shows the geoelectrical section along profile G-H. The section suggests that the subsurface along the profile is made up of three, four and five layers at VESD2, VESD3 and VESD1 respectively. The first layer has resistivity values ranging from 20 to 150 ohm-m, with an average thickness of 0.6m. The second layer has resistivity range between 463 to 230 ohm-m. The third layer has resistivity values between 170 to 520 ohm-m. The absence of this layer at VESD1 may indicate the degree of weathering in the area. The fourth layer has resistivity value of 420 ohm-m and only present at VESD3. This may be an indication that some areas are highly weathered than others.

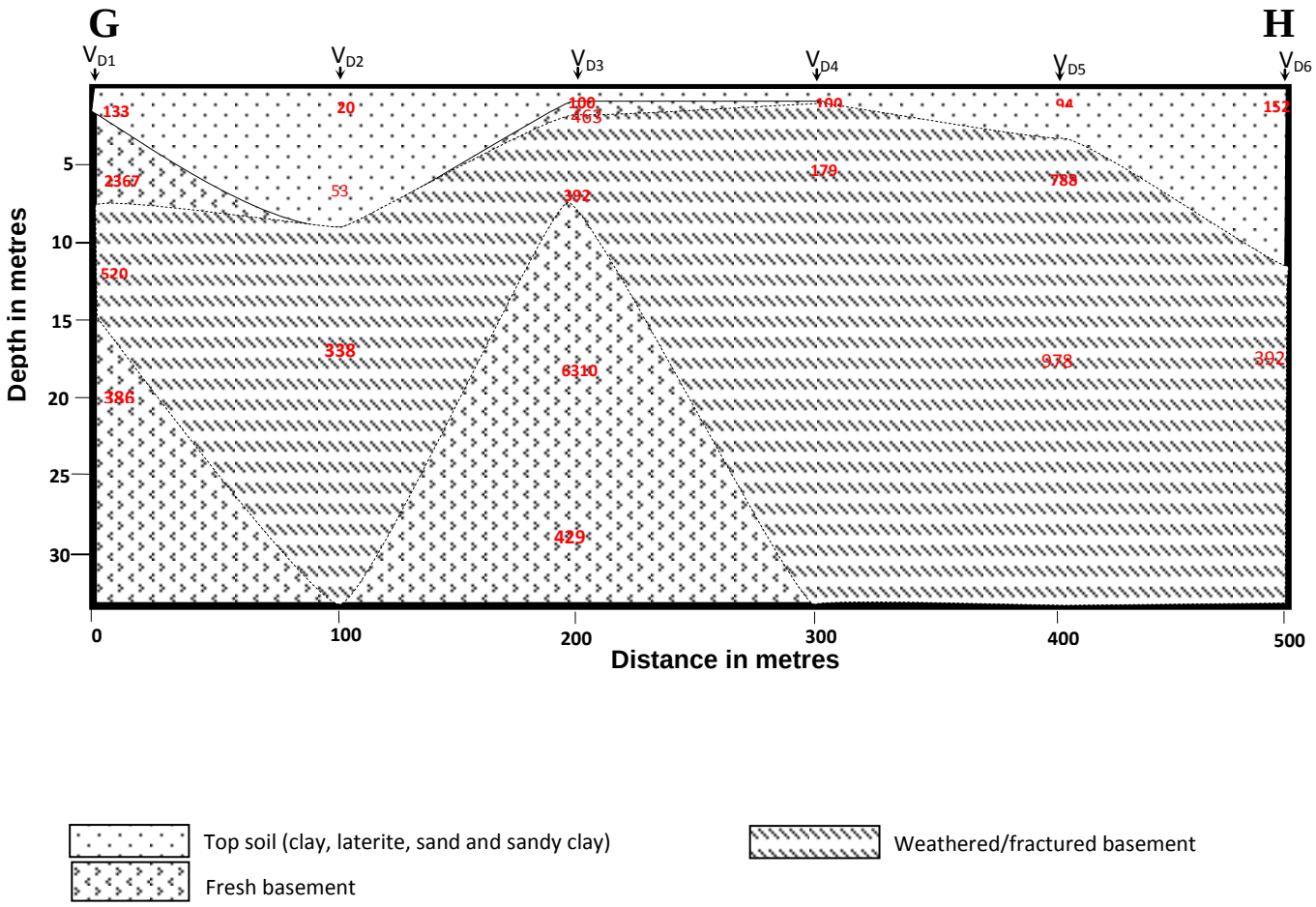


Figure 5.8 Geoelectric section along profile G-H

5.5.5 Profile I-J

Figure 5.9 shows the geological section along profile I-J. The subsurface has four layers at VESE1 and three layers at VES E2. The first layer runs throughout the profile with resistivity values ranging from 70 to 120 ohm-m with an average thickness of 4.3m. Underlying the above layer is a formation having the resistivity range between 41 to 254 ohm-m. The thickness is highly variable but thickest at VES E1. The third layer has resistivity value of 674 ohm-m with thickness of 14.2m and only present at VES E1. This indicates the degree of weathering at VES E1. The fourth layer has resistivity value greater than 800 ohm-m, and this is probably the fresh basement.

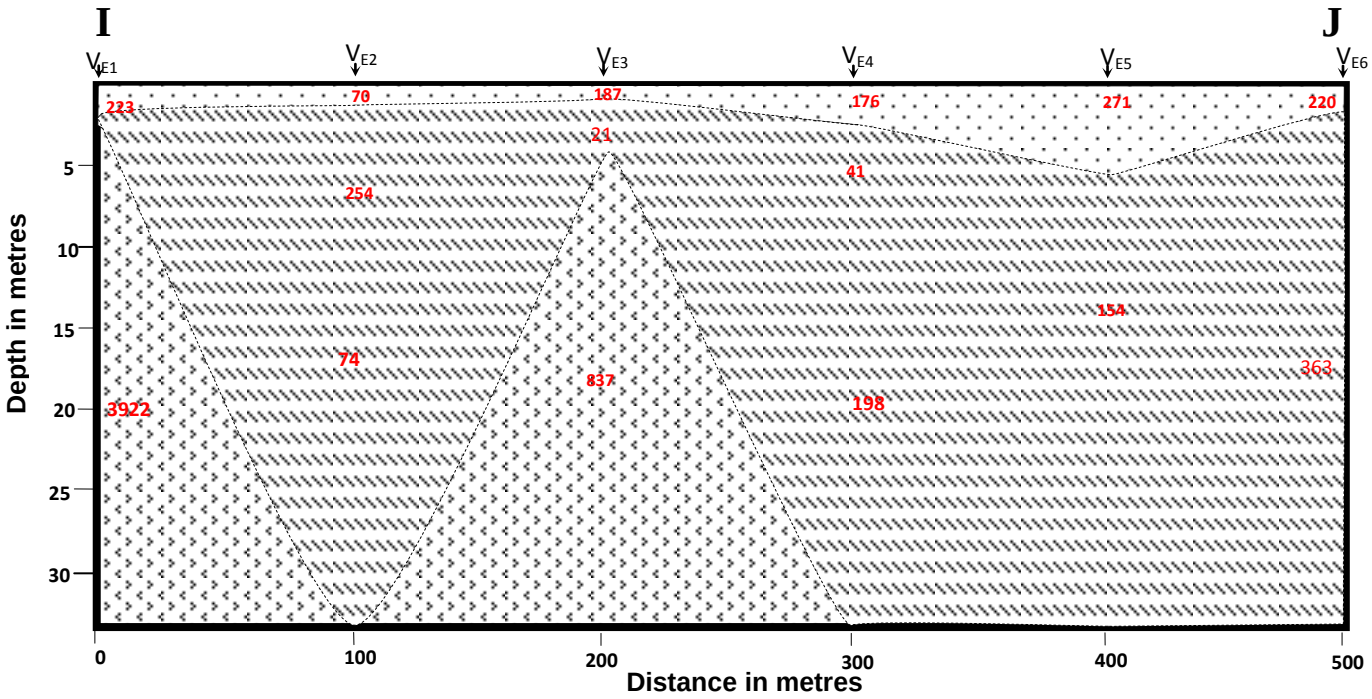


Figure 5.9 Geoelectric section along profile I-J

5.6 Overburden Resistivity Contour Map

The map was produced by contouring the resistivity values of the overburden at all the 30 VES points within the study area. The map and the surface plot are shown in figure 18 and figure 19 respectively. A contour interval of 20ohm-m was used for the map. The resistivity values of the top soil vary between 55 to 367ohm-m. The N-W area has lower resistivity value.

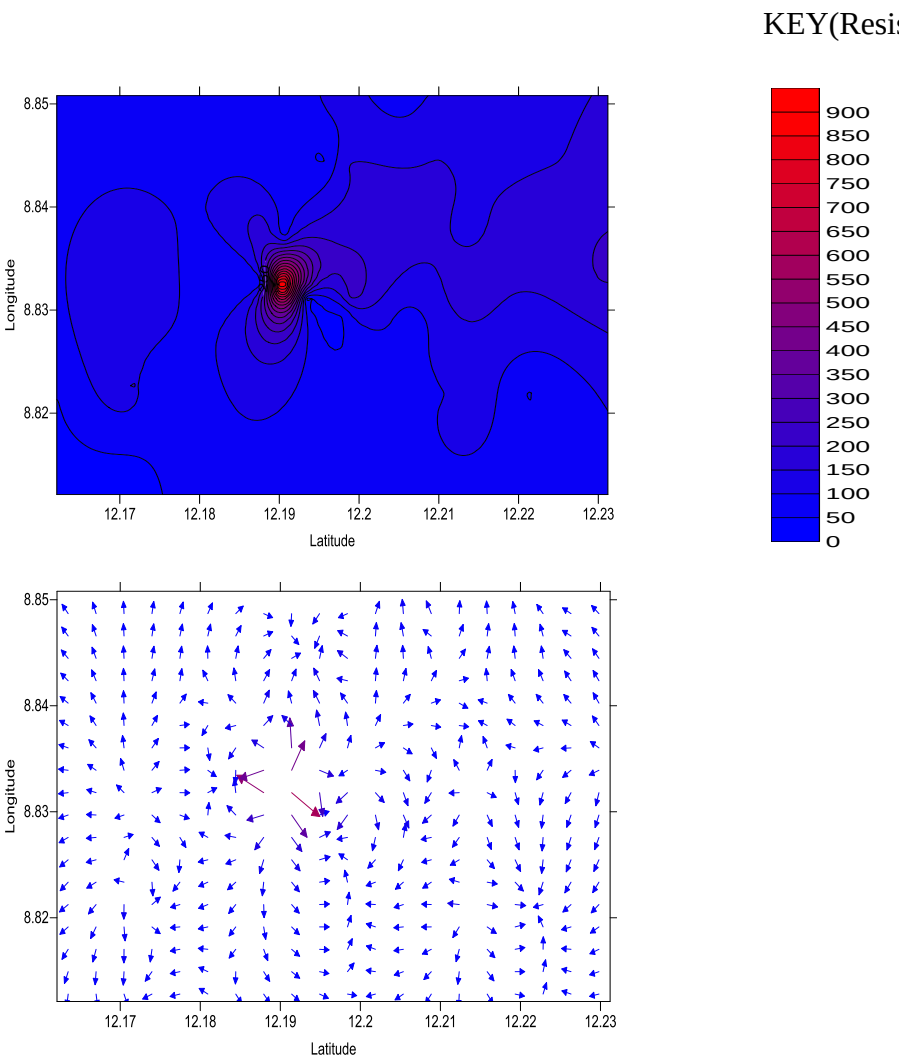


Figure 5.10 Map of resistivity of Overburden (contour interval 20ohm-metres)

5.7 Aquifer Thickness Contour Map

In the basement complex the main aquifer system include the weathered and the fractured rocks. However, other formations such as gravel layer may serve as underground water bearing layer . The aquifer thickness map was produced from the interpreted data of the weathered/fractured layer thickness for all the VES points and at interval of 2m. The map (Figure 5.10) and the

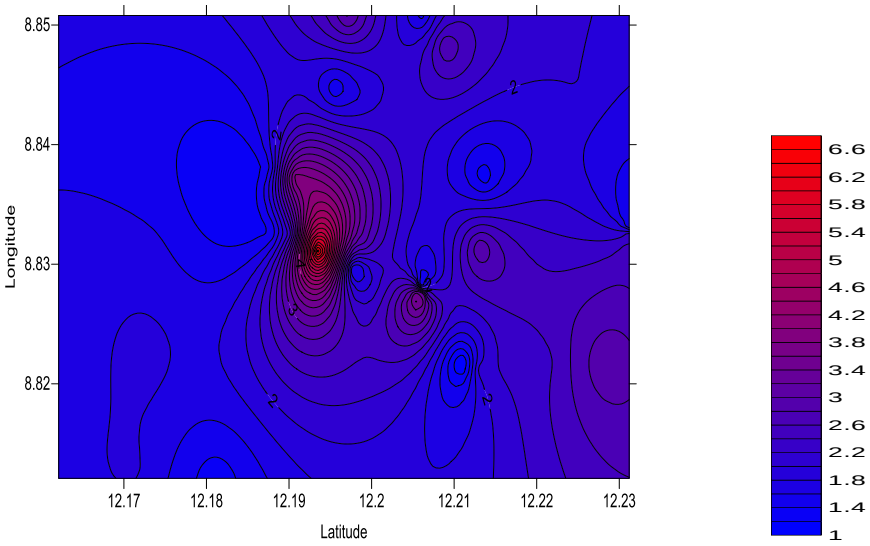
surface plot (figure5.11) show the variation of aquifer thickness from one place to another. The aquifer thickness varies from 1 to 35m with an average of 18m. The aquifer thickness and depth to basement maps correlate as the low thickness values correspond to areas of shallow basement. The larger thickness values correlate with the basement depressions.

5.8 Depth to Basement Map

The depth to basement contour map for the study area is shown in fig. 5.11a. The map was produced from the interpreted depth to fresh basement at each VES station. This map gave a good picture of the basement topography in area. The map shows that the basement topography is rugged or undulating being deeper at some points and shallower at other points. The depth to basement ranges from 11m around VES01 to 85m around VES23. The map also reveals a linear structure (VES05, 21, 22 and VES23,) which trends in the NE-SW direction. This structure suggests a basement depression at these points.

5.9 Thickness of Overburden

The aquifer thickness map was produced by contouring all the thicknesses of the first layer at each VES point at an interval of 0.5m. The map is shown in figure 5.11b. The map indicates the variation of the topsoil thickness from one place to another. The thickness varies from 0.2 to 5.2m, with an average of 2.1m. The lowest thickness is at VES27 where the depth to basement is as low as 10m.



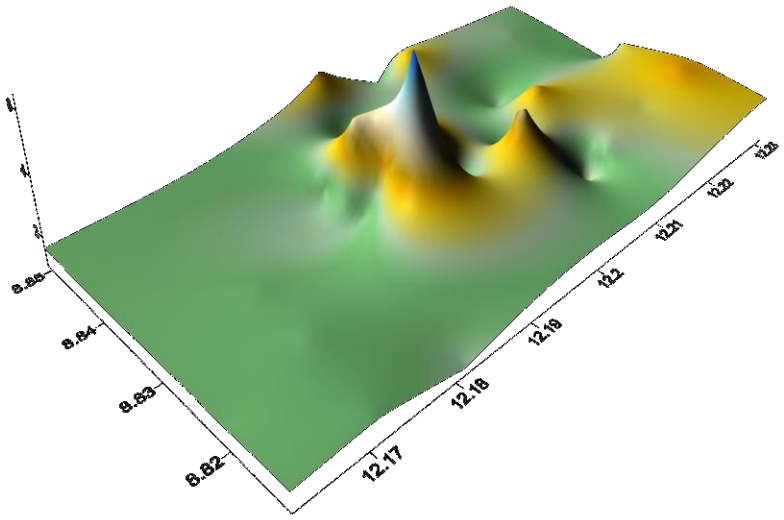


Fig 5.11 :Over burden thickness map of the area

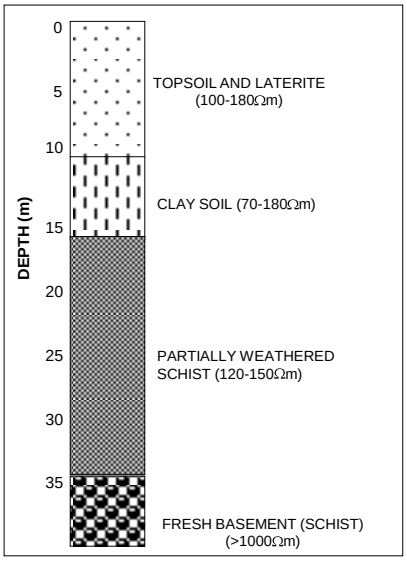


Figure 3: Geological Well-Log obtained by Kano state water resources company

Table 6: Resistivity Values Adopted for this Work

ROCK TYPES	RESISTIVITY RANGES(Ωm)
Clay	1 – 120
Sand, gravel and lateritic soil	100 – 180
Weathered basement	20 – 400
Fractured basement	135 – 900
Weathered laterite	500 – 1000
Fresh basement	>1000

Chapter Six

Summary , Conclusion and Recommendations

6.1 Summary

The study area revealed about four layers. This consists of the topsoil, lateritic clay, weathered layer and fresh basement. The top soil has thickness value that ranges between 0.6 and 1.4m, while its resistivity value varies from 20.0 to 357 ohm-m. suggesting that the topsoil is predominantly sand and sandy clay.

The Resistivity type curves associated with the study area were of three to five layer types. The predominant layers within the survey area were: the top soil consisting of laterites, clay and fadama loam having resistivity value range of 20-367 ohm-m, with an average thickness of 1m. Underlying this layer is the weathered basement consisting of sand, with resistivity value range of 76-980 ohm-m with thickness not exceeding 25m. The next is the fractured basement with resistivity ranging from 150-800 ohm-m for both profile A-B and C-D. Underneath the fractured layer is the Fresh basement of infinite thickness and resistivity values ranging from 500 to greater than 1000 ohm-m.

Weathered/Fractured basement serves as principal aquifer in the study area with an average thickness of 18m. The variations of resistivity at different depths enabled the aquifer saturation to be determined. The section 10m below the ground level fall within low resistivity value range and can be classified to be most suitable for groundwater exploitation, either through dug well or borehole. The VES points A2, A3, A5, B1, B5, C4, D3, D5, E1, E2, and E6 are recommended as areas of high groundwater potentials. The existing and functional borehole at VES A1 has large aquifer thickness and low depth to water table. This is true when compared with the borehole log obtained from National Water Institute, Kaduna. This finding is in agreement with Kumar (2002) who stated that there is a correlation between the depth to basement and depth to water table, on the other hand, the non-functional borehole at VESE6 has small aquifer thickness and large depth to water table which could be a possible reason why the borehole failed not up to two years after it has been drilled.

6.2 Conclusion

The geoelectric sections for profile A-B and C-D shows that the area is underlain by rocks of different lithological compositions, namely: top soil consisting of laterites, clay and fadama loam, weathered basement (sandy), fractured and fresh basement rocks.

The geoelectric sections were carefully examined to see the regions where extensive weathering occurs along fractures. These together with information obtained from such maps as; depth to basement, aquifer thickness led to the conclusion that: VES points A2, A3 , A5, B1 , B5, C4, D3, D4, D5, E1, E2, E3, and E6 have the greatest groundwater potentials in the area and are suitable for dug well, and borehole development. VES points A5, D4, D5 and E1 fall on the linear region of the basement depression shown on the depth to basement map. Also the thickness of the weathered/fractured basement beneath the region was found to be considerably large about 18m

The aquifer thickness map of the study area (Figure 4.10) suggests that the thickness of the weathered and/fractured basement layer vary from 1-21,m. Areas with low resistivity values at great depth imply structural disturbance which may have been cause by fracturing of the bedrock.

The basement rocks with resistivity values greater than 2000 ohm-m are less weathered and contain little or no quantity of ionize water.

6.3 Recommendations

The electrical resistivity method is a reconnaissance tool. However it is also suitable for the detailed study of problem areas that have been selected using other techniques, such as Gravity Method, Electromagnetic Method (EM), or resistivity traversing. But to obtain the best results in the future, a combination of this method is suggested. Two-dimensional electrical surveys should be carried out in conjunction with seismic or GPR surveys as they provide complementary and clear information about the subsurface. Before any geotechnical construction takes place in any important and fundamental subsurface investigation, the geophysical measurement should be utilized first. This will help to identify areas which are liable to possess structural defects during and after the construction and necessary precaution(s) will be available in the design/construction

plan. This will minimize and reduce the cost of rehabilitation and construction of failed structures.

Finally, future work should be extended beyond the limit of the profiles and better understanding of the target area and also 2D and 3D resistivity survey should be undertaken within the area under investigation.

References

Adamu, A.G., 1973. Basement geology of Zaria, Samaru Area. An unpublished B.Sc. project, Geology Department Ahamadu Bello University, Zaria.

Akintorinwa, O.J. and Adeusi, F.A., 2009. Integration of Geophysical and geotechnical investigation of a proposed Lecture Room Complex at the Federal University of Technology, Akure,SW, Nigeria. Ozean Journal of Science, 2(3), 996-1009.

Badmus B.S, Ayolabi E.A, Olowofeh J.A, Adisa S.A. and Oyekunle T.O., 2005. Current Variation in Electric Resistivity probing using Wenner and Schlumberger arrays in a basement terrain. Journal of Geophysics, volume 2,pp118-125.

Barnes, H.E.,(1952). Soil Mechanics in Road Construction. Butter and Tanner Publishing Company, Great Britain, pp 23-25.

Bobachev, A.A, Igor N.M and Vladimir A.S.,2001. Ipi2win user guide. Moscow State University, Geological Faculty, Department of Geophysics. Geoscan-MLTD.

Burger, D.C. and Burger H.R.,1992. Exploration Geophysics for the shallow subsurface, Prentice Hall,pp445-446.

Chiemeke, C.C. and Osazuwa, I.B., (2007). Application of seismic refraction tomography for complex subsurface imaging in central Northern Nigeria; Nigeria Journal of physics, Vol.16,pp1-8.

Clark, N.J.,1960. Elements of petroleum reservoirs SPE of AIME. Vol.23,p8.

Eigbefo, C.,1978. Hydrogeological of the Kubanni Drainage Basin, Zaria. Unpublished M.Sc. thesis, Department of Physics, Ahmadu Bello University, Zaria.

Esse,O., Oyedele, K.F., Ogagaurue, D.O., 2011. Groundwater potential Evaluation using surface Geophysics at Oru-Imope, southwestern Nigeria. European Journal of Scientific Research. ISSN 1450-2160, Volume 63, No 4, pp515-522.

Farouk, A.U., 2001. Geoelectric investigation of the groundwater potential in the Institute for Agricultural Research Farm, Zaria. Unpublished M.Sc. Thesis, Department of Physics, Ahmadu Bello University, Zaria.

Gholam, R.L. and Nad, M.N., 2005. Geoelectrical investigation for the assessment of groundwater condition: A case study of Annals of Geophysics. Volume 48,No6, P 937-944.

Grant, N.K.,1969. The late Precambrian to early Paleozoic Pan-African Orogeny in Ghana,Togo, Dahomey and Nigeria. Geology Society. Am.Bull., Volume 80, pp45-56.

Griffiths, D.H, Turnbull J. and Olayinka, A.I., 1990. Two- dimensional resistivity mapping with a computer-controlled array. First Break, 8, 121-129.

Joda, F.O., 1990. The establishment of a local gravity network for Zaria area. Unpublished M.Sc. Thesis, Department of Physics, Ahmadu Bello University, Zaria.

Kearey P., Michael B. and Ian H., 2002. An introduction to Geophysical Exploration 3 edition, Blackwell Publishing, Malden,M.A,, United State of America.

Keller, G.V. and Frischknecht, F.C., 1966. Electrical Methods in Geophysical Prospecting. Pergamon Press Inc., Oxford.

Koefoed, O., 1979. Geosounding principles1: Resistivity sounding measurements. Elsevier Science Publication, Amsterdam.

Kogbe, C.A., 1989. Geology of Nigeria. Rock view (Nigeria) Limited, plot 1234, Zaramaganda, Jos, Nigeria. PP348-350.

Kumar. D, 2002. Assessment of Natural groundwater recharge in Upper Ganga Canal Command Area. Journal of Application of Hydrology, Vol.15(4), 13-20.

Loke M.H., 1994. The inversion of two-dimensional resistivity data. Unpublished, PhD thesis, University of Birmingham, United Kingdom.

Louise, P., 2002. Application of electrical and electromagnetic methods for environmental and geotechnical, surveys in Geophysics,23,101-132. University of Utah, Energy and Geoscience Institute Salt Lake City, Utah.84112.

McCurry, P., 1970. The geology of degree sheet 21, Zaria. Unpublished M.Sc. thesis, Department of Geography, Ahmadu Bello University, Zaria.

McCurry. P, 1976. The geology of Precambrian to lower paleozoic rocks of northwestern Nigeria. A review in Kogbe, C.A. (Ed), Geology of Nigeria. Elizabeth Publishing Company, Lagos, pp15-39.

Moore, W., 1945. An empirical method of interpretation of Earth Resistivity measurement, transactions of American Institute of Mining and Metallurgical Engineers: Volume164, pp197-223.

Obaje, N.G., 2009. Lecture notes in Earth Science,Vol. 120, Geology and Mineral Resources of Nigeria. www.Springer.com/series/772.

Ogunmola, J.K., Adeofun, C.O., Ogbole, J.O., Goki, N.G., and Ohia, J.A.,(2008). The use of Nigeria SAT-1 and GIS in assessing the mineral potential of raffin-gabbas, north central Nigeria. Middle-east Journal of Scientific Research,3(3), 164-170, IDOSI Publication.

Olowu, D., 1967. Preliminary investigation of the groundwater conditions in Zaria sheet 102 SW: *GSN* report No 1462.

Osazuwa, I.B., Chiemeke, C.C., Abdullahi, N.K.and Akaolisa, C.C., 2008. *Improved depth of penetration of Geoelectric imaging in a confined Area Using Refraction Tomography*. Journal of Environmental Hydrology, Volume 16, pp 3-8. On the World Wide Web at http://www.hydroweb.com.

Oseji, J.O., 2002. The aquifer systems of Ndokwa Land, Delta state. IJRAAS Publication 5(3), p 26 published in Department of Physics, Delta State University, Abraka Delta State.

Osemeikhan J.E.A. and Asokhia M.B., 1994. Applied Geophysics for engineers and Geologists. 1Ed Santos Service Limited, Lagos.

Ososami, I.A., 1968. Assessment of the groundwater in the Kubanni Valley. Unpublished M.Sc. Thesis, Department of Physics,Ahmadu Bello University, Zaria.

Oyewoye, M.O., 1964. Geology of the Nigerian Basement Complex, Journal of Nigeria mining, Geological and Metallurgical Society, volume8, pp87-102.

Russ, W., 1957. The geology of part of Niger, Zaria and Sokoto provinces with special reference to the occurrence of gold, Bulletin: Geological Survey, Nigeria, No 27, p42.

Telford, W.M, Geldart ,L.P, Sheriff, R.E. and Keys, D.A., 1976. Applied Geophysics, Cambridge University Press, London. 860pp.

Tokarski, A., 1972. Heterogeneous Terrace Arrangement, west of Ahmadu Bello University Zaria, Occasional paper No1, Department of Geology, Ahmadu Bello University, Zaria.

Truswell, J.F. and Cope. R.N., 1963. The geology of parts of Niger and Zaria provinces, Northern Nigeria: Geology Survey of Nigeria. Bulletin 29,pp52.

Umar, F.A., 2001. Geoelectric investigation of the groundwater potential in the Institute of Agricultural Research (IAR) farm, Samaru, Zaria. Unpublished M.Sc. thesis, Department of Physics, Ahmadu Bello University, Zaria.

Wright, J.B. and McCurry,P., 1970. The geology of Nigeria sheet 102 SW, Zaria and its regions. Edited by M.J. Mortimore. Department of Geography,occasional paper No4, Ahmadu Bello University, Zaria.

Zohdy A.A.R., 1989. A new method for the automatic interpretation of Schlumberger and Wenner sounding curves: Geophysics, Volume 54, pp9-39.

Appendix I

Field data

AB/2 (m)	MN/2 (m)	K-FACTOR (m)	RES (ohms)	APP RES (ohm-m)
1.5	1.0	1.964	94.2	185
2.0	1.0	4.712	21.7	102
3.0	1.0	12.568	13.2	166
4.5	1.0	30.243	8.6	260
7.0	1.0	75.408	6.6	498
10.0	1.0	155.529	4.1	638
15.0	2.0	173.596	7.1	1233
20.0	2.0	311.058	5.3	1649
30.0	2.0	703.808	2.2	1548
45.0	2.0	1587.496	0.9	1429
60.0	2.0	2824.658	0.5	1412
70.0	2.0	3845.808	0.3	1154

VES A1

AB/2 (m)	MN/2 (m)	K-FACTOR (m)	RES (ohms)	APP RES (ohm-m)
1.5	1.0	1.964	37.0	73
2.0	1.0	4.712	13.3	63
3.0	1.0	12.568	3.9	49
4.5	1.0	30.243	1.7	51
7.0	1.0	75.408	0.8	60
10.0	1.0	155.529	0.5	78
15.0	2.0	173.596	0.8	139
20.0	2.0	311.058	0.6	187
30.0	2.0	703.808	0.6	422
45.0	2.0	1587.496	0.4	635
60.0	2.0	2824.658	0.3	847
70.0	2.0	3845.808	0.3	1153

VES A2

AB/2 (m)	MN/2 (m)	K-FACTOR (m)	RES (ohms)	APP RES (ohm-m)
1.5	1.0	1.964	11.8	23
2.0	1.0	4.712	5.7	27
3.0	1.0	12.568	1.9	24
4.5	1.0	30.243	1.7	51
7.0	1.0	75.408	0.8	60
10.0	1.0	155.529	0.5	78
15.0	2.0	173.596	0.5	87
20.0	2.0	311.058	0.2	62
30.0	2.0	703.808	0.1	70
45.0	2.0	1587.808	0.0	0
60.0	2.0	2824.658	0.1	283
70.0	2.0	3845.808	0.1	385

VES A3

AB/2 (m)	MN/2 (m)	K-FACTOR (m)	RES (ohms)	APP RES (ohm-m)
1.5	1	1.964	34.7	68
2.0	1	4.712	15.6	74
3.0	1	12.568	6.9	87
4.5	1	30.243	2.7	82
7.0	1	75.408	1.4	106
10.0	1	155.529	0.6	93
15.0	2	173.596	6.7	1163
20.O	2	311.058	0.9	280
30.0	2	703.808	2.0	1408
45.0	2	1587.496	10.2	16193
60.0	2	2824.658	0.3	847
70.0	2	3845.808	0.2	769

VES A4

AB/2 (m)	MN/2 (m)	K-FACTOR (m)	RES (ohms)	APP RES (ohm-m)
1.5	1.0	1.964	46.8	92
2.0	1.0	4.712	18.1	85
3.0	1.0	12.568	8.1	102
4.5	1.0	30.243	3.1	94
7.0	1.0	75.408	0.8	60
10.0	1.0	155.529	0.4	62
15.0	2.0	173.596	0.8	139
20.0	2.0	311.058	0.5	156
30.0	2.0	703.808	0.2	141
45.0	2.0	1587.496	0.1	159
60.0	2.0	2824.658	0.7	1977
70.0	2.0	3845.808	0.1	385

VES A5

AB/2 (m)	MN/2 (m)	K-FACTOR (m)	RES (ohms)	APP RES (ohm-m)
1.5	1.0	1.964	75.3	148
2.0	1.0	4.712	4.9	23
3.0	1.0	12.568	3.0	38
4.5	1.0	30.243	2.6	79
7.0	1.0	75.408	0.9	68
10.O	1.0	155.529	1.2	187
15.O	2.0	173.596	1.1	191
20.O	2.0	311.058	0.9	280
30.O	2.0	703.808	0.8	563
45.O	2.0	1587.496	0.7	1111
60.O	2.0	2824.658	0.7	1977
70.O	2.0	3845.808	0.7	2692

VES A6

AB/2 (m)	MN/2 (m)	K-FACTOR (m)	RES (ohms)	APP RES (ohm-m)
1.5	1.0	1.964	85.3	167
2.0	1.0	4.712	20.7	98
3.0	1.0	12.568	6.5	82
4.5	1.0	30.243	2.2	67
7.0	1.0	75.408	0.7	53
10.0	1.0	155.529	0.4	62
15.0	2.0	173.596	30.8	5347
20.0	2.0	311.058	9.8	3048
30.0	2.0	703.808	0.3	211
45.0	2.0	1587.496	0.0	0
60.0	2.0	2824.658	0.1	283
70.0	2.0	3845.808	0.2	769

VES B1

AB/2 (m)	MN/2 (m)	K-FACTOR (m)	RES (ohms)	APP RES (ohm-m)
1.5	1.0	1.964	2.4	5
2.0	1.0	4.712	7.1	34
3.0	1.0	12.568	9.7	122
4.5	1.0	30.243	3.9	117
7.0	1.0	75.408	2.1	158
10.0	1.0	155.529	1.5	233
15.0	2.0	173.596	3.0	521
20.0	2.0	311.058	1.3	404
30.0	2.0	703.808	0.6	422
45.0	2.0	1587.496	0.4	635
60.0	2.0	2824.658	0.2	565
70.0	2.0	3845.808	0.1	385

VESB2

AB/2 (m)	MN/2 (m)	K-FACTOR (m)	RES (ohms)	APP RES (ohm-m)
1.5	1.0	1.964	488.0	958
2.0	1.0	4.712	232.0	1093
3.0	1,0	12.568	78.9	992
4.5	1.0	30.243	26.9	814
7,0	1.0	75.408	5.6	422
10.0	1.0	155.529	1.0	156
15.0	2.0	173.596	0.9	156
20.0	2.0	311.058	0.6	187
30.0	2.0	703.808	0.5	352
45.0	2.0	1587.496	0.1	159
60.0	2.0	2824.658	0.5	1412
70.0	2.0	3845.808	0.2	769

VES B3

AB/2 (m)	MN/2 (m)	K-FACTOR (m)	RES (ohms)	APP RES (ohm-m)
1.5	1.0	1.964	79.7	157
2.0	1.0	4.712	29.7	140
3.0	1.0	12.568	6.4	80
4.5	1.0	30.243	2.3	70
7.0	1.0	75.408	0.8	60
10.0	1.0	155.529	0.3	47
15.0	2.0	173.596	5.3	920
20.0	2.0	311.058	11.4	3546
30.0	2.0	703.808	1.3	915
45.0	2.0	1587.496	1.6	2540
60.0	2.0	2824.658	2.1	5932
70.0	2.0	3845.808	11.6	44611

VES B4

AB/2 (m)	MN/2 (m)	K-FACTOR (m)	RES (ohms)	APP RES (ohm-m)
1.5	1.0	1.964	68.9	135
2.0	1.0	4.712	23.0	108
3.0	1.0	12.568	7.6	96
4.5	1.0	30.243	2.7	82
7.0	1.0	75.408	1.1	83
10.0	1.0	155.529	0.5	78
15.0	2.0	173.596	0.8	139
20.0	2.0	311.058	0.3	93
30.0	2.0	703.808	0.2	141
45.0	2.0	1587.496	0.1	159
60.0	2.0	2824.658	0.2	565
70.0	2.0	3845.808	0.1	385

VES B5

AB/2 (m)	MN/2 (m)	K-FACTOR (m)	RES (ohms)	APP RES (ohm-m)
1.5	1.0	1.964	90.9	179
2.0	1.0	4.712	27.2	128
3.0	1.0	12.568	7.5	94
4.5	1.0	30.243	1.8	54
7.0	1.0	75.408	1.1	83
10.0	1.0	155.529	0.4	62
15.0	2.0	173.596	0.4	69
20.0	2.0	311.058	0.1	31
30.0	2.0	703.808	0.2	141
45.0	2.0	1587.496	0.3	476
60.0	2.0	2824.658	0.3	847
70.0	2.0	3845.808	0.1	585

VES B6

AB/2 (m)	MN/2 (m)	K-FACTOR (m)	RES (ohms)	APP RES (ohm-m)
1.5	1.0	1.964	71.7	141
2.0	1.0	4.712	26.7	126
3.0	1.0	12.568	8.7	109
4.5	1.0	30.243	2.3	70
7.0	1.0	75.408	1.0	75
10.0	1.0	155.529	0.2	31
15.0	2.0	173.596	4.9	851
20.0	2.0	311.058	5.7	1773
30.0	2.0	703.808	0.2	141
45.0	2.0	1587.496	0.1	159
60.0	2.0	2824.658	1.7	4802
70.0	2.0	3845.808	4.6	17691

VES C1

AB/2 (m)	MN/2 (m)	K-FACTOR (m)	RES (ohms)	APP RES (ohm-m)
1.5	1.0	1.964	38.5	76
2.0	1.0	4.712	7.6	36
3.0	1.0	12.568	3.5	44
4.5	1.0	30.243	1.9	58
7.0	1.0	75.408	101.0	7616
10.0	1.0	155.529	0.5	78
15.0	2.0	173.596	0.5	87
20.0	2.0	311.058	0.3	93
30.0	2.0	703.808	0.2	141
45.0	2.0	1587.496	0.1	159
60.0	2.0	2824.658	0.1	283
70.0	2.0	3845.808	0.1	385

VES C2

AB/2 (m)	MN/2 (m)	K-FACTOR (m)	RES (ohms)	APP RES (ohm-m)
1.5	1.0	1.964	0.3	1
2.0	1.0	4.712	87.7	413
3.0	1.0	12.568	48.3	607
4.5	1.0	30.243	18.8	569
7.0	1.0	75.408	9.3	701
10.0	1.0	155.529	3.3	513
15.0	2.0	173.596	2.5	434
20.0	2.0	311.058	1.4	436
30.0	2.0	703.808	0.3	211
45.0	2.0	1586.496	0.4	635
60.0	2.0	2824.658	0.1	283
70,0	2.0	3845.808	0.1	385

VES C3

AB/2 (m)	MN/2 (m)	K-FACTOR (m)	RES (ohms)	APP RES (ohm-m)
1.5	1.0	1.964	71.8	140
2.0	1.0	4.712	0.2	1
3.0	1.0	12.568	0.4	5
4.5	1.0	30.243	0.9	27
7.0	1.0	75.408	0.9	68
10.0	1.0	155.529	0.9	140
15.0	2.0	173.596	0.5	87
20.0	2.0	311.058	0.2	62
30.0	2.0	703.808	0.3	211
45.0	2.0	1587.496	0.1	159
60.0	2.0	2824.658	0.2	565
70.0	2.0	3845.808	0.3	1154

VES C4

AB/2 (m)	MN/2 (m)	K-FACTOR (m)	RES (ohms)	APP RES (ohm-m)
1.5	1.0	1.964	52.8	104
2.0	1.0	4.712	20.6	97
3.0	1.0	12.568	11.3	142
4.5	1.0	30.243	5.2	157
7.0	1.0	75.408	0.8	60
10.0	1.0	155.529	0.5	78
15.0	2.0	173.596	11.6	2014
20.0	2.0	311.058	7.3	2271
30.0	2.0	703.808	2.0	1408
45.0	2.0	1587.496	0.9	1429
60.0	2.0	2824.658	0.8	2260
70.0	2.0	3845.808	0.4	1538

VES C5

AB/2 (m)	MN/2 (m)	K-FACTOR (m)	RES (ohms)	APP RES (ohm-m)
1.5	1.0	1.964	82.3	162
2.0	1.0	4.712	0.2	1
3.0	1.0	12.568	0.3	4
4.5	1.0	30.243	0.6	18
7.0	1.0	75.408	0.9	68
10.0	1.0	155.529	0.9	140
15.0	2.0	173.596	0.6	104
20.0	2.0	311.058	0.4	124
30.0	2.0	703.808	0.3	211
45.0	2.0	1587.496	0.2	318
60.0	2.O	2824.658	0.1	283
70.0	2.0	3845.808	0.1	385

VES C6

AB/2 (m)	MN/2 (m)	K-FACTOR (m)	RES (ohms)	APP RES (ohm-m)
1.5	1.0	1.964	73.9	145
2.0	1.0	4.712	32.1	151
3.0	1.0	12.568	13.2	166
4.5	1.0	30.243	7.9	239
7.0	1.0	75.408	6.1	460
10.0	1.0	155.529	3.9	607
15.0	2.O	173.596	8.3	1441
20.0	2.0	311.058	6.5	2022
30.0	2.0	703.808	2.3	1619
45.0	2.0	1587.496	0.9	1429
60.0	2.0	2824.658	0.7	1977
70.0	2.0	3845.808	0.7	2692

VES D1

AB/2 (m)	MN/2 (m)	K-FACTOR (m)	RES (ohms)	APP RES (ohm-m)
1.5	1.0	1.964	10.3	20
2.0	1.0	4.712	5.2	25
3.0	1.0	12.568	2.1	26
4.5	1.0	30.243	1.3	39
7.0	1.0	75.408	0.9	68
10.0	1.0	155.529	0.4	62
15.0	2.0	173.529	0.3	52
20.0	2.0	311.058	0.3	93
30.0	2.0	703.808	0.4	282
45.0	2.0	1587.496	0.1	159
60.0	2.0	2824.658	0.1	283
70.0	2.0	3845.808	0.1	385

VES D2

AB/2 (m)	MN/2 (m)	K-FACTOR (m)	RES (ohms)	APP RES (ohm-m)
1.5	1.0	1.964	46.9	92
2.0	1.0	4.712	37.9	179
3.0	1.0	12.568	67.2	845
4.5	1.0	30.243	12.4	375
7.0	1.0	75.408	5.0	377
10.0	1.0	155.529	3.5	544
15.0	2.0	173.596	3.1	538
20.0	2.0	311.058	2.9	902
30.0	2.0	703.808	1.1	774
45.0	2.0	1587.496	2.1	3334
60.0	2.0	2824.658	0.1	282
70.0	2.0	3845.808	0.9	3461

VES D3

AB/2 (m)	MN/2 (m)	K-FACTOR (m)	RES (ohms)	APP RES (ohm-m)
1.5	1.0	1.964	27.9	55
2.0	1.0	4.712	14.7	69
3.0	1.0	12.568	5.9	74
4.5	1.0	30.243	3.6	109
7.0	1.0	75.408	2.3	173
10.0	1.0	155.529	0.7	109
15.0	2.0	173.596	1.1	191
20.0	2.0	311.058	0.8	249
30.0	2.0	703.808	0.1	70
45.0	2.0	1587.496	0.2	318
60.0	2.0	2824.658	0.1	283
70.0	2.0	3845.808	0.1	385

VES D4

AB/2 (m)	MN/2 (m)	K-FACTOR (m)	RES (ohms)	APP RES (ohm-m)
1.5	1.0	1.964	56.1	110
2.0	1.0	4.712	12.3	58
3.0	1.0	12.568	7.0	88
4.5	1.0	30.243	4.1	124
7.0	1.0	75.408	0.7	53
10.0	1.0	155.529	0.4	62
15.0	2.0	173.596	0.2	35
20.0	2.0	311.058	0.2	62
30.0	2.0	703.808	1.0	704
45.0	2.0	1587.496	0.2	318
60.0	2.0	2824.658	0.6	1695
70.0	2.0	3845.808	0.9	3461

VES D5

AB/2 (m)	MN/2 (m)	K-FACTOR (m)	RES (ohms)	APP RES (ohm-m)
1.5	1.0	1.964	75.3	148
2.0	1.0	4.712	15.4	73
3.0	1.0	12.568	7.3	92
4.5	1.0	30.243	2.1	64
7.0	1.0	75.408	0.9	68
10.0	1.0	155.529	0.3	47
15.0	2.0	173.596	0.1	17
20.0	2.0	311.058	0.3	93
30.0	2.0	703.808	0.1	70
45.0	2.0	1587.496	0.1	159
60.0	2.0	2824.658	0.1	283
70.0	2.0	3845.581	0.3	1154

VES D6

AB/2 (m)	MN/2 (m)	K-FACTOR (m)	RES (ohms)	APP RES (ohm-m)
1.5	1.0	1.964	136.5	268
2.0	1.0	4.712	54.7	257
3.0	1.0	12.568	15.8	199
4.5	1.0	30.243	5.8	175
7.0	1.0	75.408	4.4	332
10.0	1.0	155.529	1.6	249
15.0	2.0	173.596	8.5	1476
20.0	2.0	311.058	5.1	1586
30.0	2.0	703.808	2.7	1900
45.0	2.0	1587.496	1.6	2540
60.0	2.0	2824.658	0.6	1695
70.0	2.0	3845.808	0.6	2308

VES E1

AB/2 (m)	MN/2 (m)	K-FACTOR (m)	RES (ohms)	APP RES (ohm-m)
1.5	1.0	1.964	37.9	74
2.0	1.0	4.712	7.3	34
3.0	1.0	12.568	4.0	50
4.5	1.0	30.243	1.3	39
7.0	1.0	75.408	1.2	91
10.0	1.0	155.529	1.3	202
15.0	2.0	173.596	0.5	87
20.0	2.0	311.058	0.5	156
30.0	2.0	703.808	0.4	282
45.0	2.0	158.496	0.1	159
60.0	2.0	2824.658	0.1	283
70.0	2.0	3845.808	0.1	385

VES E2

AB/2 (m)	MN/2 (m)	K-FACTOR (m)	RES (ohms)	APP RES (ohm-m)
1.5	1.0	1.964	67.4	132
2.0	1.0	4.712	32.1	151
3.0	1.0	12.568	7.3	92
4.5	1.0	30.243	0.8	24
7.0	1.0	75.408	0.2	15
10.0	1.0	155.529	0.1	16
15.0	2.0	173.596	0.2	35
20.0	2.0	311.058	0.3	93
30.0	2.0	703.808	0.1	70
45.0	2.0	1587.496	1.0	159
60.0	2.0	2824.658	1.0	283
70.0	2.0	3845.808	0.3	1154

VES E3

AB/2 (m)	MN/2 (m)	K-FACTOR (m)	RES (ohms)	APP RES (ohm-m)
1.5	1.0	1.964	83.0	163
2.0	1.0	4.712	23.9	113
3.0	1.0	12.568	14.8	186
4.5	1.0	30.243	10.1	306
7.0	1.0	75.408	0.4	30
10.0	1.0	155.529	0.6	93
15.0	2.0	173.596	0.2	35
20.0	2.0	311.058	0.2	62
30.0	2.0	703.808	0.1	70
45.0	2.0	1587.496	0.1	159
60.0	2.0	2824.658	0.1	283
70.0	2.0	3845.808	0.1	385

VES E4

AB/2 (m)	MN/2 (m)	K-FACTOR (m)	RES (ohms)	APP RES (ohm-m)
1.5	1.0	1.964	67.9	133
2.0	1.0	4.712	34.2	161
3.0	1.0	12.568	12.0	151
4.5	1.0	30.243	10.0	302
7.0	1.0	75.408	23.0	1734
10.0	1.0	155.529	0.9	140
15.0	2.0	173.596	0.3	52
20.0	2.0	311.058	0.1	31
30.0	2.0	703.808	0.1	70
45.0	2.0	1587.496	0.1	159
60.0	2.0	2824.658	0.1	285
70.0	2.0	3845.808	0.1	385

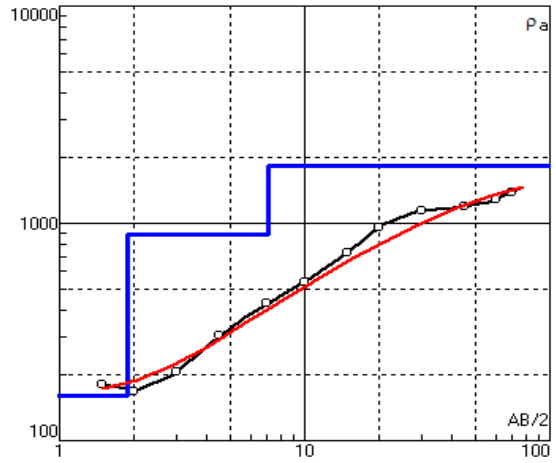
VES E5

AB/2 (m)	MN/2 (m)	K-FACTOR (m)	RES (ohms)	APP RES (ohm-m)
1.5	1.0	1.964	101.4	199
2.0	1.0	4.712	78.9	372
3.0	1.0	12.568	67.9	853
4.5	1.0	30.243	23.1	699
7.0	1.0	75.408	9.7	732
10.0	1.0	155.529	6.3	980
15.0	2.0	173.596	7.1	1233
20.0	2.0	311.058	0.7	218
30.0	2.0	703.808	0.9	633
45.0	2.0	1587.496	0.5	794
60.0	2.0	2824.658	0.2	565
70.0	2.0	3845.808	0.1	385

VES E6

Appendix II

The resistivity Graph



Field curve
Synthetic curve
Model

ρ- Layer Resistivity in Ωm

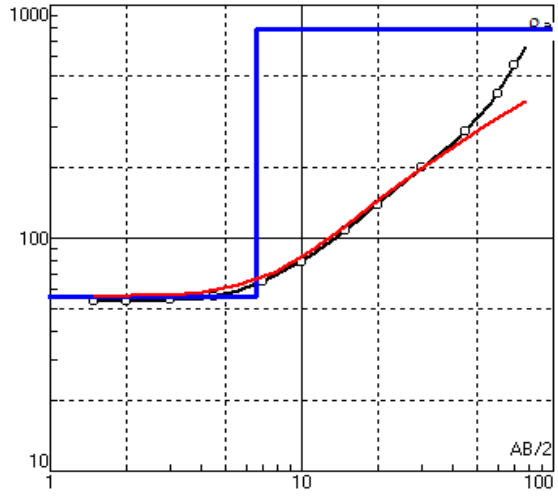
h- Layer thickness in metres

d- depth to interface in metres

N-layer number

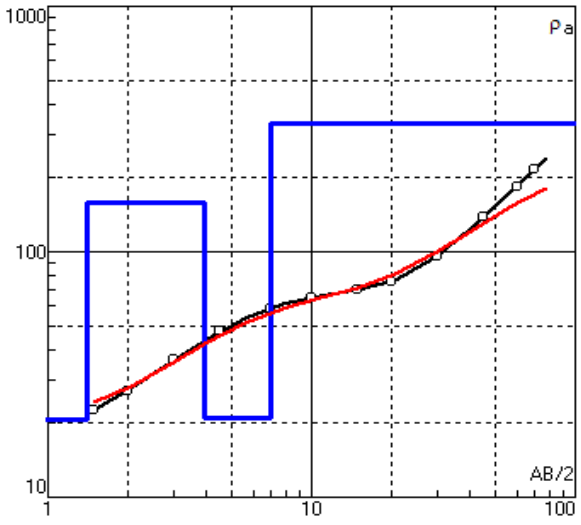
N	ρ	h	d
1	161	1.89	1.89
2	888	5.21	7.11
3	1839		

VES A1



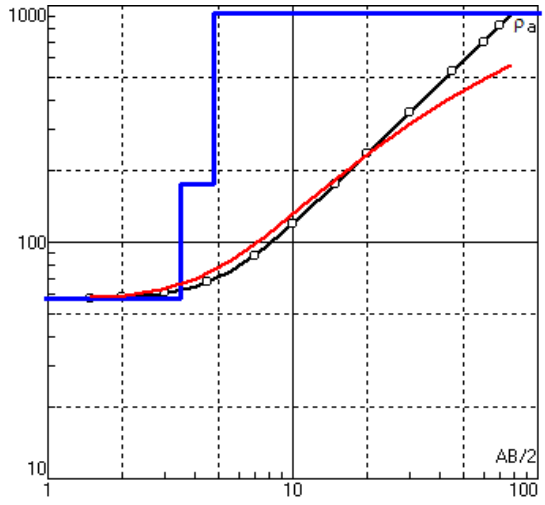
N	ρ	h	d
1	56	6.6	6.6
2	788		

VES A2



N	ρ	h	d
1	20	1.41	1.41
2	159	2.49	3.89
3	21	3.12	7.01
4	333		

VES A3



Field curve

Synthetic curve

Model

ρ- Layer Resistivity in Ωm

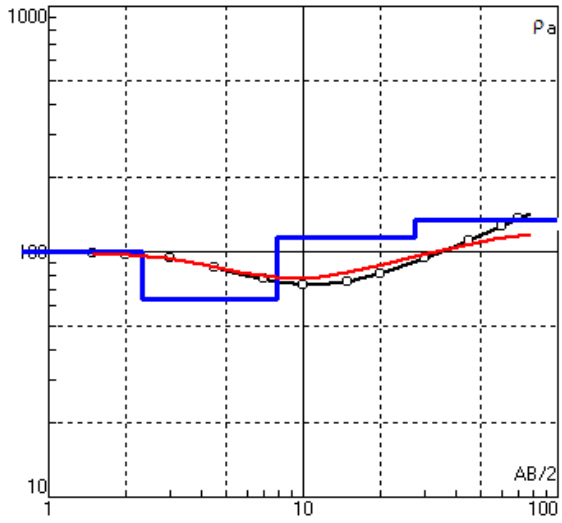
h- Layer thickness in metres

d- depth to interface in metres

N-layer number

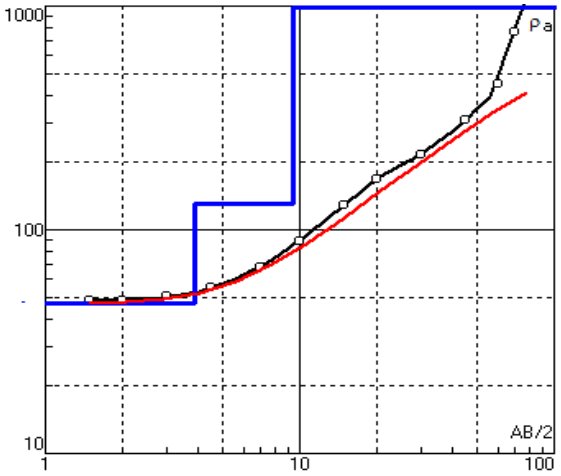
N	ρ	h	d
1	57	3.48	3.48
2	175	1.28	4.76
3	928		

VES A4



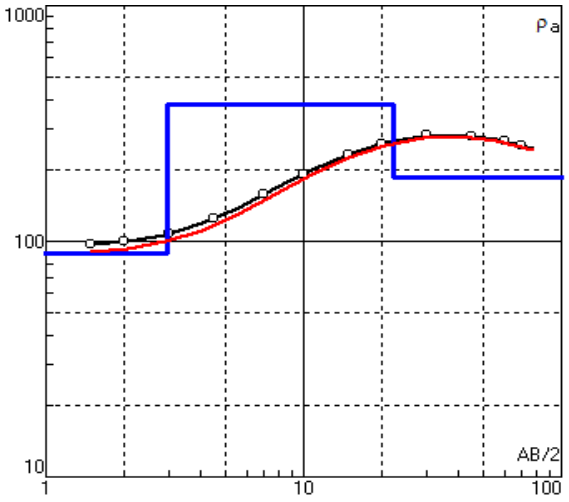
N	ρ	h	d
1	99	2.33	2.33
2	64	5.55	7.88
3	114	19.6	27.5
4	135		

VES A5



N	ρ	h	d
1	46	3.86	3.86
2	130	5.56	9.42
3	1046		

VES A6



Field curve

Synthetic curve

Model

ρ- Layer Resistivity in Ωm

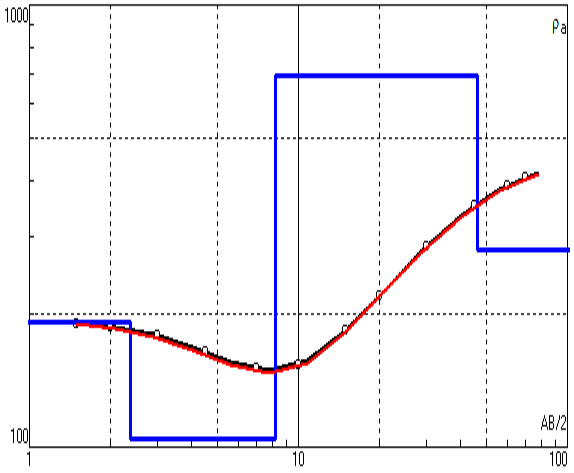
h- Layer thickness in metres

d- depth to interface in metres

N-layer number

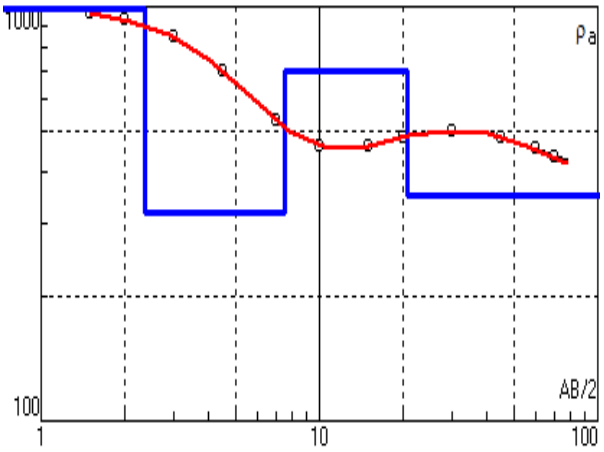
N	ρ	h	d
1	89	2.96	2.96
2	381	19.3	22.3
3	187		

VES B1



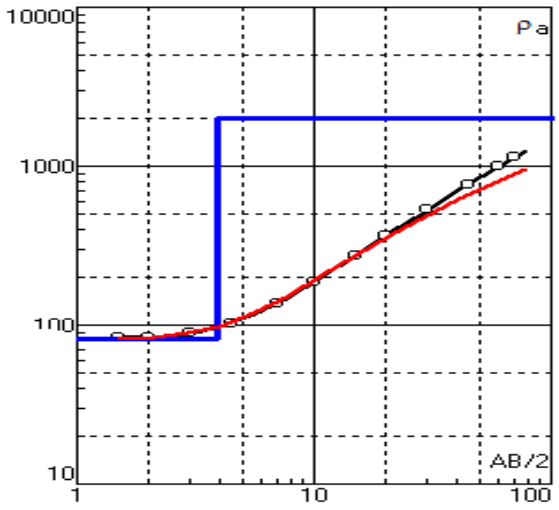
N	ρ	h	d
1	192	2.37	2.37
2	104	5.87	8.24
3	689	37.94	46.18
4	278		

VES B2



N	ρ	h	d
1	985.3	2.37	2.37
2	318.6	5.17	7.54
3	700.1	13.17	20.71
4	348.3		

VES B3



Field curve

Synthetic curve

Model

ρ- Layer Resistivity in Ωm

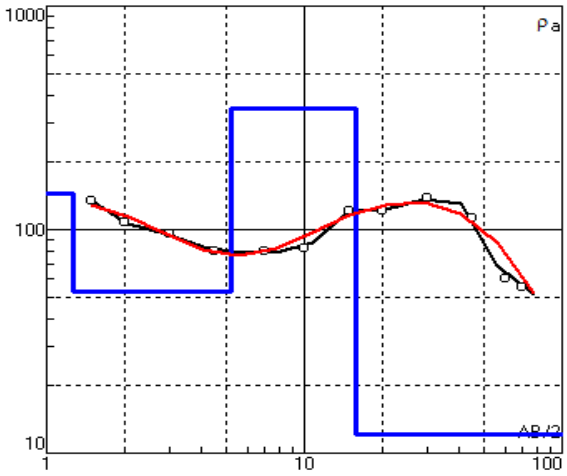
h- Layer thickness in metres

d- depth to interface in metres

N-layer number

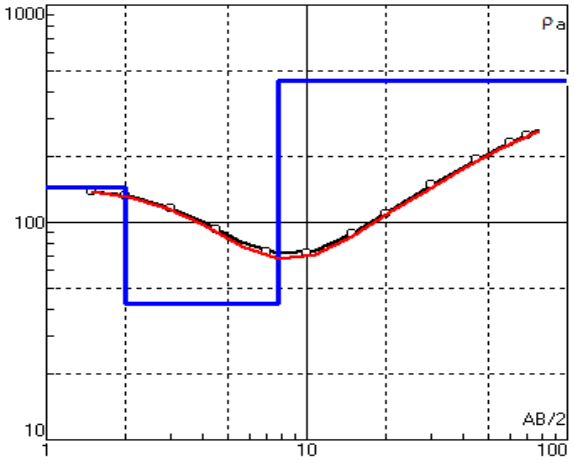
N	ρ	h	d
1	81	3.9	3.9
2	2000		

VES B4



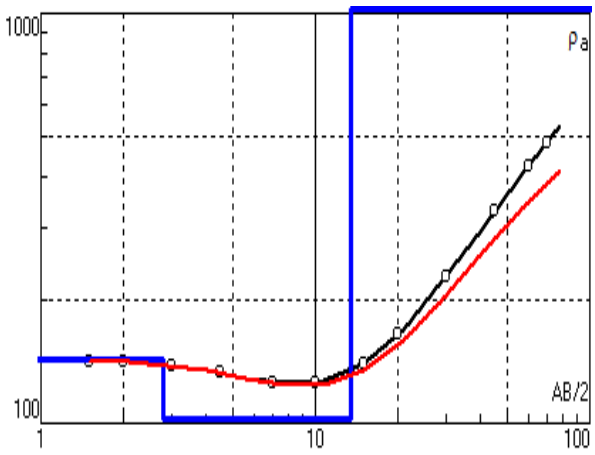
N	ρ	h	d
1	144	1.27	1.27
2	53	4.1	5.37
3	351	10.7	16.1
4	12		

VES B5



N	ρ	h	d
1	145	2.01	2.01
2	42	5.76	7.77
3	448		

VES B6



Field curve

Synthetic curve

Model

ρ- Layer Resistivity in Ωm

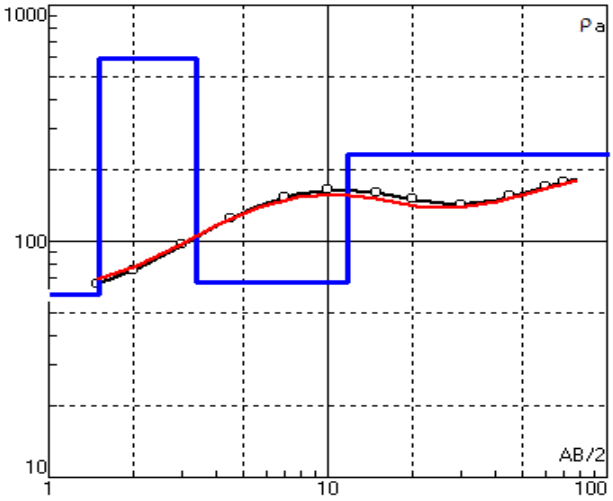
h- Layer thickness in metres

d- depth to interface in metres

N-layer number

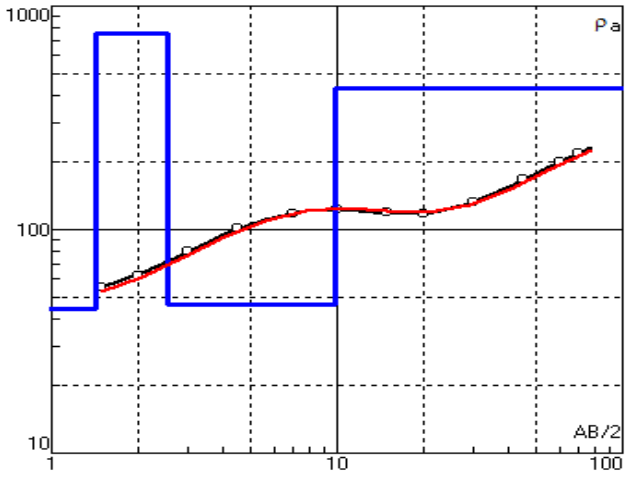
N	ρ	h	d
1	143	2.8	2.8
2	103	10.7	13.5
3	1024		

VES C1



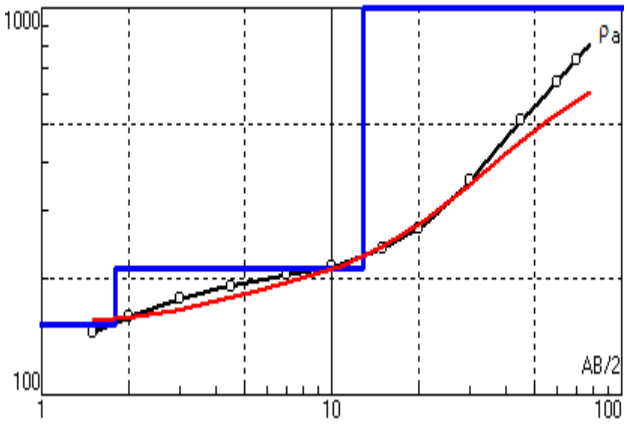
N	ρ	h	d
1	60	1.52	1.52
2	595	1.87	3.38
3	67	8.43	11.8
4	233		

VES C2



N	ρ	h	d
1	44	1.43	1.43
2	754	1.12	2.55
3	46	7.31	9.86
4	429		

VES C3



Field curve

Synthetic curve

Model

ρ- Layer Resistivity in Ωm

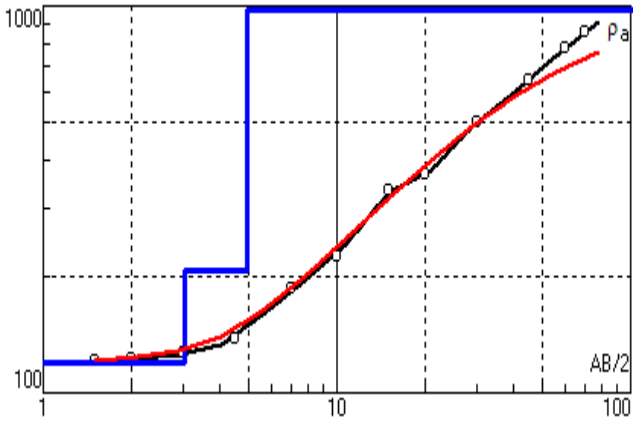
h- Layer thickness in metres

d- depth to interface in metres

N-layer number

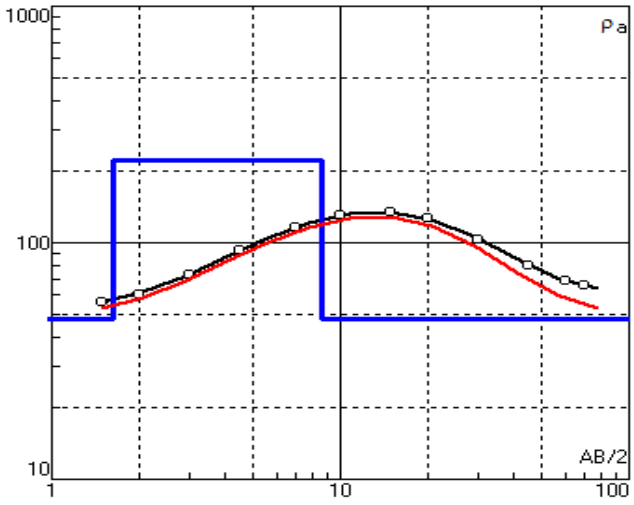
N	ρ	h	d
1	152	1.79	1.79
2	211	11.1	12.8
3	1000		

VES C4



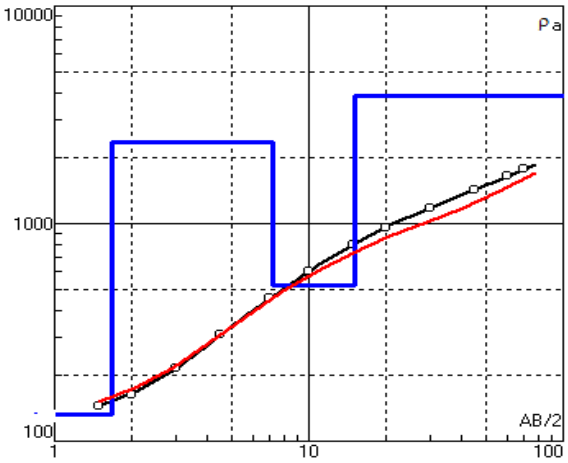
N	ρ	h	d
1	120	3.05	3.05
2	207	1.91	4.96
3	976		

VES C5



N	ρ	h	d
1	48	1.63	1.63
2	223	6.99	8.62
3	48		

VES C6



Field curve

Synthetic curve

Model

ρ- Layer Resistivity in Ωm

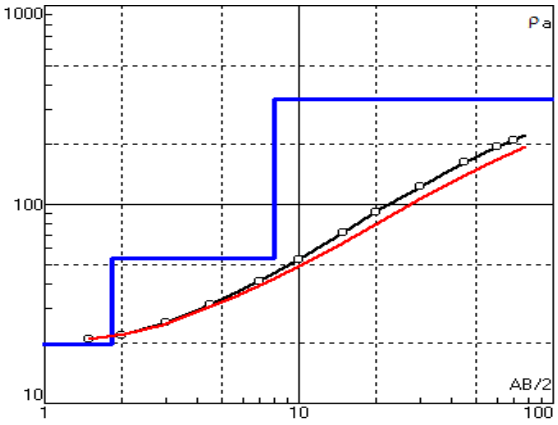
h- Layer thickness in metres

d- depth to interface in metres

N-layer number

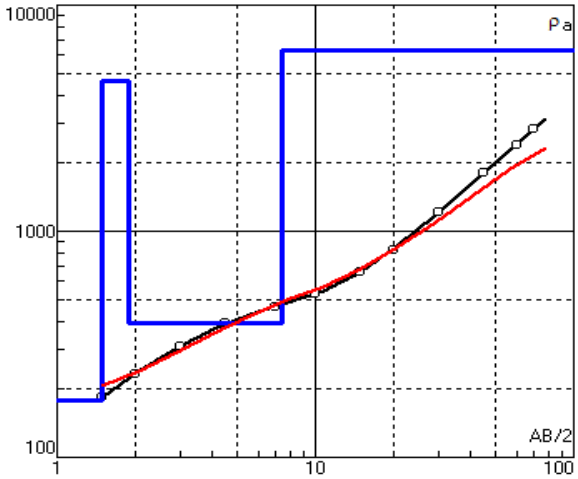
N	ρ	h	d
1	133	1.69	1.69
2	2367	5.55	7.24
3	520	7.97	15.2
4	3865		

VES D1



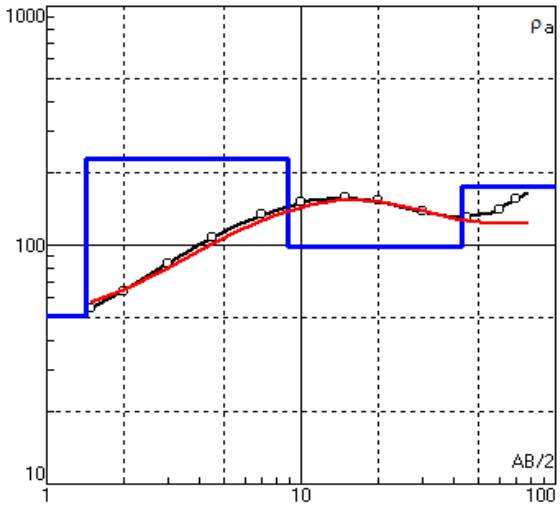
N	ρ	h	d
1	20	1.84	1.84
2	53	6.28	8.12
3	338		

VES D2



N	ρ	h	d
2	4635	0.41	1.9
3	392	5.54	7.44
4	6310		

VES D3



Field curve
Synthetic curve
Model

ρ- Layer Resistivity in Ωm

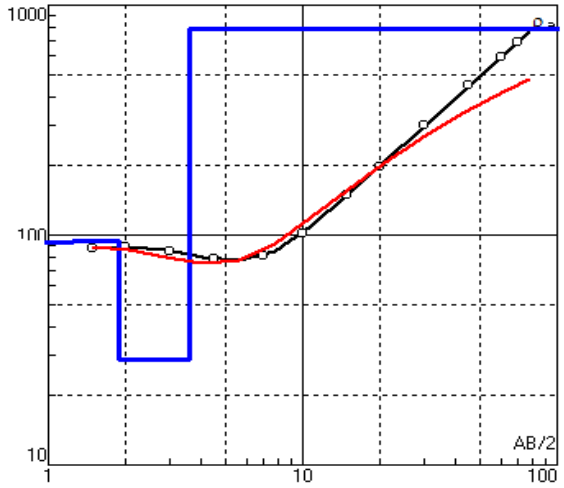
h- Layer thickness in metres

d- depth to interface in metres

N-layer number

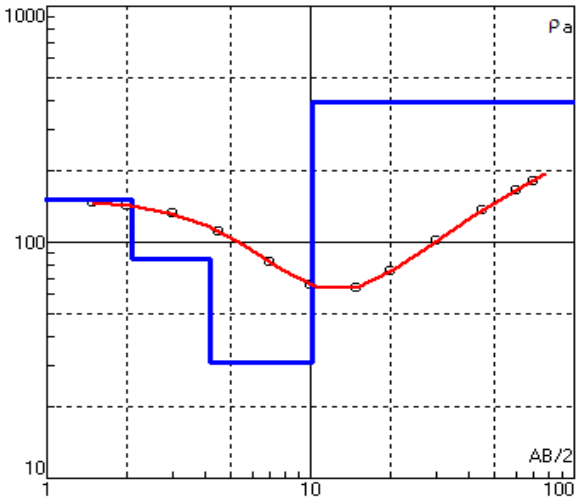
N	ρ	h	d
1	50	1.43	1.43
2	229	7.45	8.88
3	98	34.2	43.1
4	176		

VES D4



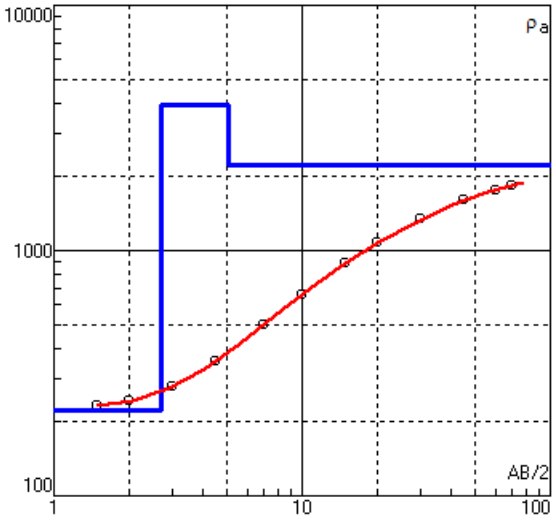
N	ρ	h	d
1	92.8	1.26	1.26
2	94.2	0.625	1.88
3	28.7	1.69	3.57
4	788		

VES D5



N	ρ	h	d
1	152	2.1	2.1
2	84	2.06	4.16
3	40	5.99	10.1
4	392		

VES D6



Field curve

Synthetic curve

Model

ρ- Layer Resistivity in Ωm

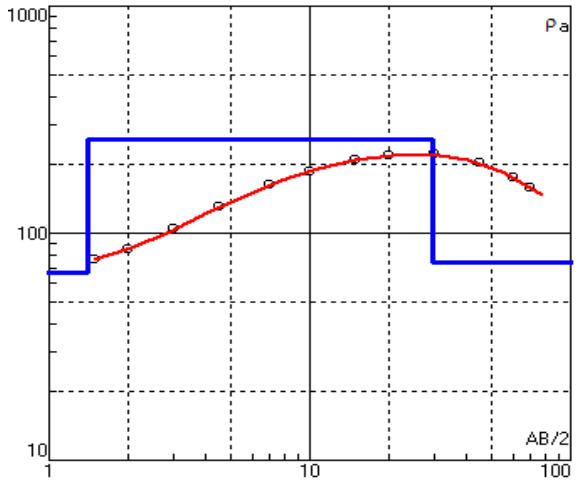
h- Layer thickness in metres

d- depth to interface in metres

N-layer number

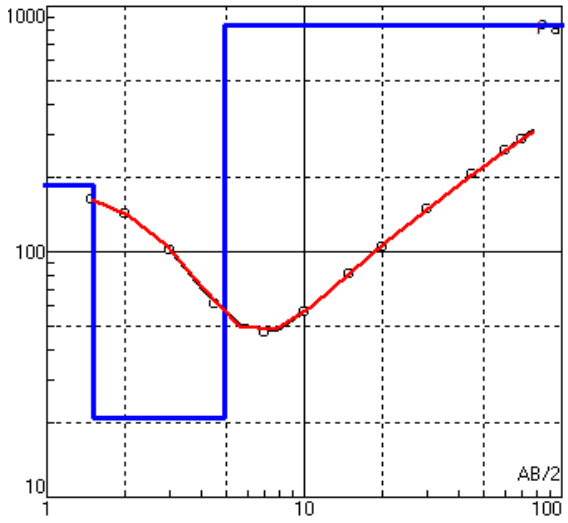
N	ρ	h	d
1	223	2.71	2.71
2	3922	2.42	5.13
3	2230		

VES E1



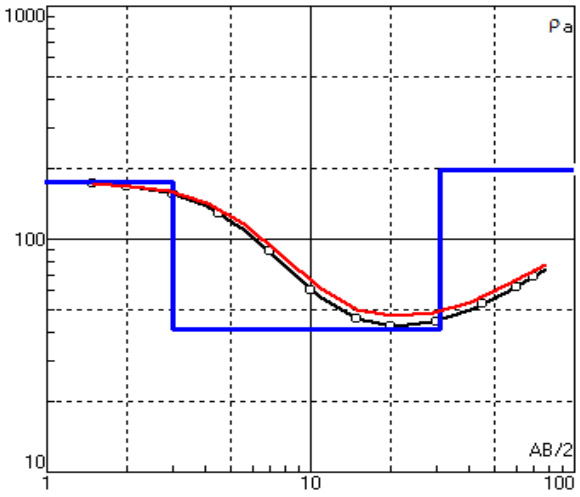
N	ρ	h	d
1	70	1.41	1.41
2	259	28.2	29.6
3	74		

VES E2



N	ρ	h	d
1	187	1.52	1.52
2	21	3.39	4.91
3	837		

VES E3



Field curve

Synthetic curve

Model

ρ- Layer Resistivity in Ωm

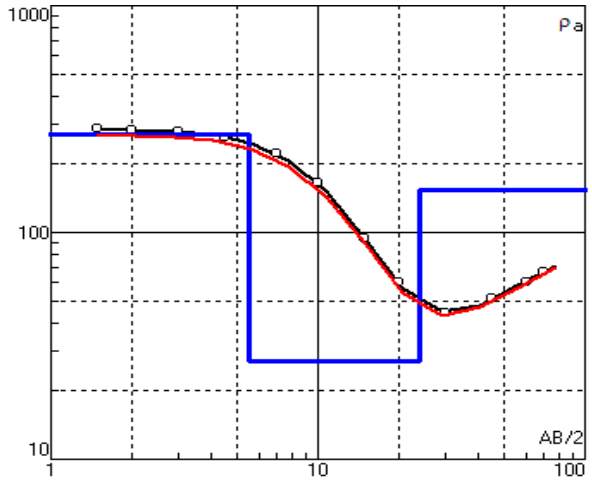
h- Layer thickness in metres

d- depth to interface in metres

N-layer number

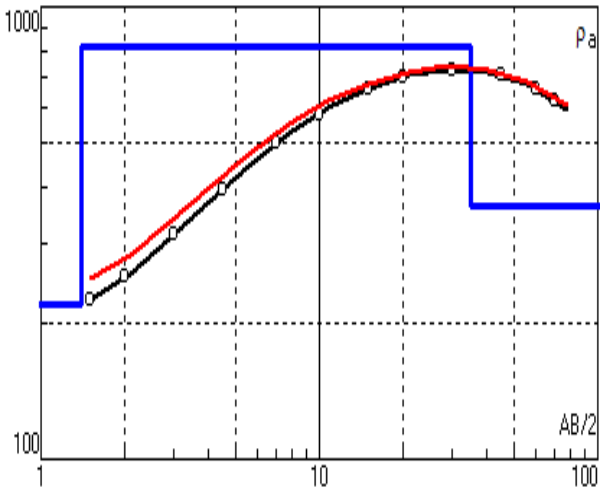
N	ρ	h	d
1	176	3	3
2	41	28	31
3	198		

VES E4



N	ρ	h	d
1	271	5.5	5.5
2	27	18.5	24
3	154		

VES E5



N	ρ	h	d
1	220	1.4	1.4
2	820	33.7	35.1
3	363		

VES E6